



Aalborg Universitet

AALBORG UNIVERSITY  
DENMARK

## Review of Laterally Loaded Monopiles Employed as the Foundation for Offshore Wind Turbines

Sørensen, Søren Peder Hyldal; Brødbæk, Kristian Thoustrup; Møller, Martin; Augustesen, Anders Hust

*Publication date:*  
2012

*Document Version*  
Early version, also known as pre-print

[Link to publication from Aalborg University](#)

*Citation for published version (APA):*  
Sørensen, S. P. H., Brødbæk, K. T., Møller, M., & Augustesen, A. H. (2012). *Review of Laterally Loaded Monopiles Employed as the Foundation for Offshore Wind Turbines*. Department of Civil Engineering, Aalborg University. DCE Technical reports No. 137

### General rights

Copyright and moral rights for the publications made accessible in the public portal are retained by the authors and/or other copyright owners and it is a condition of accessing publications that users recognise and abide by the legal requirements associated with these rights.

- Users may download and print one copy of any publication from the public portal for the purpose of private study or research.
- You may not further distribute the material or use it for any profit-making activity or commercial gain
- You may freely distribute the URL identifying the publication in the public portal -

### Take down policy

If you believe that this document breaches copyright please contact us at [vbn@aub.aau.dk](mailto:vbn@aub.aau.dk) providing details, and we will remove access to the work immediately and investigate your claim.

# **Review of laterally loaded monopiles employed as the foundation for offshore wind turbines**

**Søren Peder Hyldal Sørensen  
Kristian Thoustrup Brødbæk  
Martin Møller  
Anders Hust Augustesen**

Aalborg University  
Department of Civil Engineering  
Geotechnical Engineering Research Group

**DCE Technical Report No. 137**

# **Review of laterally loaded monopiles employed as the foundation for offshore wind turbines**

by

Søren Peder Hyldal Sørensen  
Kristian Thoustrup Brødbæk  
Martin Møller  
Anders Hust Augustesen

February 2012

© Aalborg University

## **Scientific Publications at the Department of Civil Engineering**

*Technical Reports* are published for timely dissemination of research results and scientific work carried out at the Department of Civil Engineering (DCE) at Aalborg University. This medium allows publication of more detailed explanations and results than typically allowed in scientific journals.

*Technical Memoranda* are produced to enable the preliminary dissemination of scientific work by the personnel of the DCE where such release is deemed to be appropriate. Documents of this kind may be incomplete or temporary versions of papers—or part of continuing work. This should be kept in mind when references are given to publications of this kind.

*Contract Reports* are produced to report scientific work carried out under contract. Publications of this kind contain confidential matter and are reserved for the sponsors and the DCE. Therefore, Contract Reports are generally not available for public circulation.

*Lecture Notes* contain material produced by the lecturers at the DCE for educational purposes. This may be scientific notes, lecture books, example problems or manuals for laboratory work, or computer programs developed at the DCE.

*Theses* are monographs or collections of papers published to report the scientific work carried out at the DCE to obtain a degree as either PhD or Doctor of Technology. The thesis is publicly available after the defence of the degree.

*Latest News* is published to enable rapid communication of information about scientific work carried out at the DCE. This includes the status of research projects, developments in the laboratories, information about collaborative work and recent research results.

Published 2012 by  
Aalborg University  
Department of Civil Engineering  
Sohngaardsholmsvej 57,  
DK-9000 Aalborg, Denmark

Printed in Aalborg at Aalborg University

ISSN 1901-726X  
DCE Technical Report No. 137



# Review of laterally loaded monopiles employed as the foundation for offshore wind turbines

S. P. H. Sørensen<sup>1</sup>; K. T. Brødbæk<sup>2</sup>; M. Møller<sup>2</sup>; and A. H. Augustesen<sup>3</sup>

Aalborg University, February 2012

## Abstract

The monopiles foundation concept is often employed as the foundation for offshore wind turbine converters. These piles are highly subjected to lateral loads and overturning moments due to wind and wave forces. Typically monopiles with diameters of 4 to 6 m and embedded pile lengths of 15 to 30 m are necessary. In current practice these piles are normally designed by use of the  $p$ - $y$  curve method although the method is developed and verified for small-diameter, slender piles. In the present paper a review of the existing  $p$ - $y$  curve formulations for piles in sand is presented. Based on numerical and experimental studies presented in the literature, advances and limitations of the current  $p$ - $y$  curve formulations are outlined. The review focuses on the design of monopile foundations for offshore wind turbine converters.

## 1 Introduction

It is a predominating opinion that the global warming is caused by the emission of greenhouse gasses. Therefore, it is of high political interest to reduce the emission of greenhouse gasses. This can be accomplished by investments in renewable energy. Wind power is a very competitive source of renewable energy, and therefore the market for both onshore and offshore wind farms is expected to expand. In 2008, the wind energy capacity in the world was approximately 120 GW of which Europe accounted for 65 GW. In 2030, the wind energy capacity in Europe is expected to reach 400 GW corresponding to an increase of 515 % compared to the capacity in 2008. Currently, the majority

of wind turbines are placed onshore due to lower construction costs onshore than offshore. However, dense populations and built-up areas limit the number of suitable locations on land. Therefore, the development of offshore wind farms are enforced. In 2011, the offshore wind energy capacity in Europe was approximately 4 GW, while the capacity in 2030 is expected to increase to approximately 150 GW. (see [www.ewea.org](http://www.ewea.org))

Several concepts for offshore wind turbine foundations exist, for instance, monopile foundations, gravitational foundations, bucket foundations, tripods, jacket foundations, and floating foundation concepts. The choice of foundation concept primarily depends on site conditions and the dominant type of loading. At moderate water depths the most common foundation principle is monopiles, which are single steel pipe piles driven open-ended into the soil. According to LeBlanc et al. (2009) monopiles installed recently have

---

<sup>1</sup>M. Sc., Ph.D. Student in Civil Engineering, Dept. of Civil Engineering, Aalborg University, Sohngaardsholmsvej 57, 9000 Aalborg, Denmark.

<sup>2</sup>M. Sc. in Civil Engineering, COWI A/S

<sup>3</sup>M. Sc., Ph.D. in Civil Engineering, COWI A/S

diameters around 4 to 6 m and a pile slenderness ratio,  $L/D$ , around 5 where  $L$  is the embedded pile length and  $D$  is the outer pile diameter.

For offshore wind turbine foundations the serviceability and fatigue limit states are often governing for the design. The foundations should be designed such that the accumulated rotation is less than the requirements of the wind turbine producer. Often the rotation due to installation is not allowed to exceed  $0.25^\circ$  and the accumulated rotation due to loads is restricted to  $0.25^\circ$ . Furthermore, the foundation should be designed such that resonance with the rotor frequency, the blade passing frequency, and the energy rich frequency of the environmental loads is avoided. Hence, the stiffness of the foundation for offshore wind turbines is of great importance. The blade passing frequency and the rotor frequency of the wind turbine are typically in the range of 0.5-1.0 and 0.17-0.33 Hz, respectively. Monopile foundations for offshore wind turbines are typically designed such that the first natural frequency of the structure is between the blade passing frequency and the rotor frequency.

In current design of laterally loaded offshore monopiles, the winkler model approach is normally used. Further,  $p$ - $y$  curves are typically used to describe the interaction between pile and soil. A  $p$ - $y$  curve describes the non-linear relationship between the soil resistance acting against the pile wall,  $p$ , and the lateral deflection of the pile,  $y$ . Note that there in the present paper is distinguished between soil resistance,  $p$ , and ultimate soil resistance,  $p_u$ . The soil resistance is given as the reaction force per unit length acting on the pile. The ultimate soil resistance is given as the maximum value of soil resistance.

Several formulations of  $p$ - $y$  curves exist depending on the type of soil. These formulations are originally formulated to be employed in the offshore oil and gas sec-

tor. However, they are also used for offshore wind turbine foundations, although piles with significantly larger diameter and significantly smaller slenderness ratio are employed for the foundation of these.

In the present paper the formulation and implementation of  $p$ - $y$  curves for piles in sands proposed by Reese et al. (1974), O'Neill and Murchison (1983), and design regulations of organs such as the American Petroleum Institute and Det Norske Veritas API (API, 2000; and DNV, 2010) will be presented and analysed. However, alternative methods for designing laterally loaded piles have been proposed in the literature. Alternative approaches can generally be classified as follows:

- The limit state method.
- The subgrade reaction method.
- The elasticity method.
- The strain-wedge method.
- The finite element/difference method.
- Model tests

Simplest of all the methods are the limit state methods considering only the ultimate soil resistance (e.g. Hansen, 1961; Broms, 1964; Petrasovits and Award, 1972; Meyerhof et al., 1981; Prasad and Chari, 1999; and Zhang et al., 2005).

The simplest method for predicting the pile deflection is the subgrade reaction method, e.g. Reese and Matlock (1956) and Matlock and Reese (1960). In this case the soil resistance is assumed linearly dependent on the pile deflection. Small- and full-scale tests though substantiate a non-linear relationship between soil resistance and pile deflection. The subgrade reaction method must therefore be considered too simple and highly inaccurate. In addition the subgrade reaction method is

not able to predict the ultimate lateral pile resistance.

The  $p$ - $y$  curve method assumes a non-linear dependency between soil resistance and pile deflection and is therefore able to produce a more accurate solution. In both the  $p$ - $y$  curve method and the subgrade reaction method the Winkler approach, cf. section 2, is employed to calculate the lateral deflection of the pile and the internal forces in the pile. When employing the Winkler approach the pile is considered as a beam on an elastic foundation. The beam is supported by a number of uncoupled springs with spring stiffness' given by  $p$ - $y$  curves. When using the Winkler approach the soil continuity is not taken into account as the springs are considered uncoupled.

The elasticity method, e.g. Banerjee and Davis (1978), Poulos (1971), and Poulos and Davis (1980), includes the soil continuity. However, the response is assumed to be elastic. As soil is more likely to behave elasto-plastically, this elasticity method is not to be preferred unless only small strains are considered. Hence, the method is only valid for small strains and thereby not valid for calculating the ultimate lateral pile resistance.

The strain-wedge method was originally proposed by Norris (1986) and was originally able to predict the response of flexible piles exhibited to lateral loading. Since then, the model has been developed further by, for instance, Ashour et al. (1998) and Ashour and Norris (2003) such that it can account for, among others, layered soils and soil liquefaction. The strain-wedge method links the traditional Winkler approach with the three-dimensional behaviour of soils determined from triaxial tests.

Another way to deal with the soil continuity and the non-linear behaviour is to apply a three-dimensional finite element/difference model (e.g. Abdel-

Rahman and Achmus, 2005; Fan and Long, 2005; Lesny and Wiemann, 2006; Sørensen et al., 2009; Lin et al., 2010; and Sørensen et al., 2010). When applying a three-dimensional numerical model both deformations and the ultimate lateral resistance can be determined. Due to the complexity of a three-dimensional model, substantial computational power is needed and calculations are often very time consuming. Phenomena such as liquefaction and gaps between soil and pile are at present hard to handle in the models. Hence, a numerical modelling is a useful tool but the accuracy of the results is highly dependent on the applied constitutive soil models as well as the calibration of these models.

Model tests can be conducted to investigate the behaviour of laterally loaded piles. Model tests at large scale are very expensive. Hence, small-scale tests are often preferred. When conducting small-scale tests at normal stress level, the friction angle of the soil is high and Young's modulus of elasticity is low compared to the soil properties for full-scale tests. To overcome this issue, small-scale tests can be conducted in either a centrifuge or in a pressure tank in which an overburden pressure can be applied to the soil. Small-scale tests have been conducted by, for instance, Barton et al. (1983), Georgiadis et al. (1992), Verdue et al. (2003), Sørensen et al. (2009), LeBlanc et al. (2010a), LeBlanc et al. (2010b), Klinkvort and Hededal (2010), and Brødbæk et al. (2011). When conducting small-scale tests appropriate scaling laws are necessary for the scaling to full-scale. Scaling laws applicable for laterally loaded piles have been proposed by several authors (e.g. Gudehus and Hettler, 1983; Peralta and Achmus, 2010; Leblanc et al., 2010a; and Bhatlacharya et al., 2011).

In this paper the Winkler model approach and the  $p$ - $y$  curves proposed by Reese et al. (1974) and Murchison and O'Neill



(1984) are presented in detail. These  $p$ - $y$  curves are valid for piles situated in cohesionless soil materials. The limitations of the Winkler model approach and the  $p$ - $y$  curves are discussed. Further, research within the field of laterally loaded piles situated in sand is presented. The paper addresses monopile foundations for offshore wind turbines.

## 2 $p$ - $y$ curves and Winkler approach

As a consequence of the oil and gas industry's expansion in offshore platforms in the 1950s, models for designing laterally loaded piles were required. The key problem is the soil-structure interaction as the stiffness parameters of the pile,  $E_p$ , and the soil,  $E_s$ , may be well known but at the soil-pile interface the combined parameter  $E_{py}$  is governing and unknown. In order to investigate the soil-pile interaction, a number of field tests on fully instrumented flexible piles have been conducted and various expressions for various soil conditions have been derived to predict the soil pressure acting on a pile subjected to lateral loading.

Historically, the derivation of the  $p$ - $y$  curve method for piles in sand is as follows:

- Analysing the response of beams on an elastic foundation, the soil is characterised by a series of linear-elastic uncoupled springs, introduced by Winkler (1867).
- Hetenyi (1946) presents a solution to the beam on elastic foundation problem.
- McClelland and Focht (1958) as well as Reese and Matlock (1956) suggest the basic principles in the  $p$ - $y$  curve method.

- Investigations by Matlock (1970) indicates that the soil resistance in one point is independent of the pile deformation above and below that exact point.
- Tests on fully instrumented test piles in sand installed at Mustang Island are carried out in 1966 and reported by Cox et al. (1974).
- A semi-empirical  $p$ - $y$  curve expression is derived based on the Mustang Island tests, cf. Reese et al. (1974). The expression becomes the state-of-the-art in the following years.
- O'Neill and Murchison proposes a new  $p$ - $y$  curve formulation with a tangent hyperbolic shape.
- Murchison and O'Neill (1984) compare the  $p$ - $y$  curve formulations proposed by Reese et al. (1974), with the expression by O'Neill and Murchison (1983) and two simplified expressions (also based on the Mustang Island tests) by testing the formulations against a database of relatively well-documented lateral pile load tests. The formulation of O'Neill and Murchison (1983) was found to provide better results compared to the original expressions formulated by Reese et al. (1974). The expression of O'Neill and Murchison (1983) was later adopted by design regulations of organs such as the American Petroleum Institute (API) and Det Norske Veritas (DNV).

Research has been concentrated on deriving empirical (e.g. Reese et al. 1974) and "analytical" (e.g. Ashour et al. 1998)  $p$ - $y$  curve formulations for different types of soil giving the soil resistance,  $p$ , as a function of pile displacement,  $y$ , at a given point along the pile. The soil pressure at a given depth,  $x_t$ , before and during an

excitation is sketched in fig. 1b. The passive pressure on the front of the pile is increased as the pile is deflected the distance  $y_t$  while the active pressure at the back is decreased.

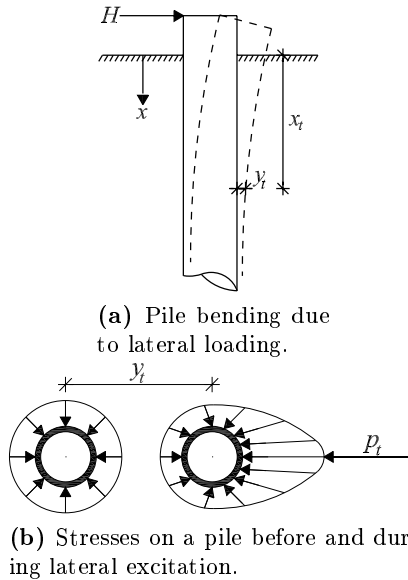


**Figure 1:** Distribution of stresses before and during lateral excitation of a circular pile.  $p_t$  denotes the net force acting on the pile at the depth  $x_t$ , after Reese and Van Impe (2001).

An example of a typical  $p$ - $y$  curve is shown in fig. 2a. The curve has an upper horizontal limit denoted by the ultimate soil resistance,  $p_u$ . The horizontal line implies that the soil has an ideal plastic behaviour meaning that no loss of shear strength occurs with increasing strain. The subgrade reaction modulus,  $E_{py}$ , at a given depth,  $x$ , is defined as the secant modulus  $p/y$ .  $E_{py}$  is thereby a function of both lateral pile deflection,  $y$ , depth,  $x$ , as well as the physical properties and load conditions.  $E_{py}$  does not uniquely represent a soil property, but is simply a convenient parameter that describes the soil-pile interaction.  $E_{py}$  decreases with increased deflection, cf. fig. 2b. A further examination of the shape of  $p$ - $y$  curves is to be found in section 3.

Since the soil-pile interaction is three-dimensional and highly nonlinear a simplified and convenient way to obtain the

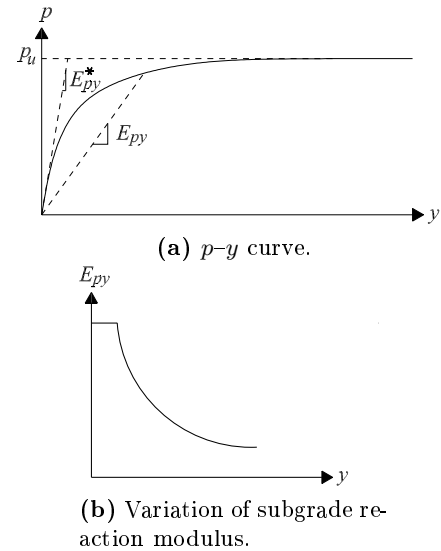


**Figure 2:** Typical  $p$ - $y$  curve and variation of the modulus of subgrade reaction at a given point along the pile, after Reese and Van Impe (2001).

soil resistance along the pile is to apply the Winkler approach in which the soil resistance is modelled as uncoupled non-linear springs with stiffness  $E_{py}$  acting on an elastic beam as shown in fig. 3. By employing uncoupled springs layered soils can conveniently be modelled.

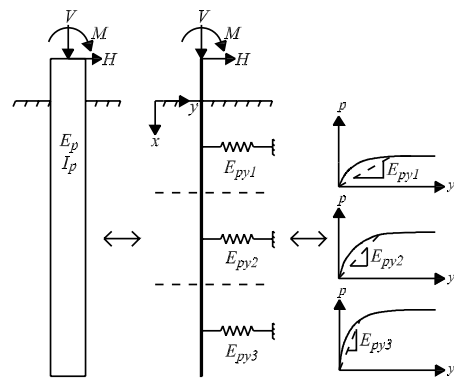


**Figure 3:** The Winkler approach with the pile modelled as an elastic beam supported by non-linear uncoupled springs.

The governing equation for beam deflection was stated by Timoshenko (1941). The equation for an infinitesimal small element,  $dx$ , located at depth  $x$ , subjected to lateral loading, can be derived from static equilibrium. The sign convention in fig. 4 is employed.  $N$ ,  $V$ , and  $M$  defines the axial force, shear force and bending moment

in the pile, respectively. The axial force,  $N$ , is assumed to act in the cross-section's centre of gravity.

Equilibrium of moments and differentiating with respect to  $x$  leads to the following equation where second order terms have been neglected:

$$\frac{d^2M}{dx^2} + \frac{dV}{dx} - N \frac{d^2y}{dx^2} = 0 \quad (1)$$

Following relations are used:

$$M = E_p I_p \kappa \quad (2)$$

$$\frac{dV}{dx} = -p \quad (3)$$

$$p(y) = -E_{py}y \quad (4)$$

$E_p$  and  $I_p$  are the Young's modulus of elasticity of the pile and the second moment of inertia of the pile, respectively.  $\kappa$  is the curvature strain of the beam element.

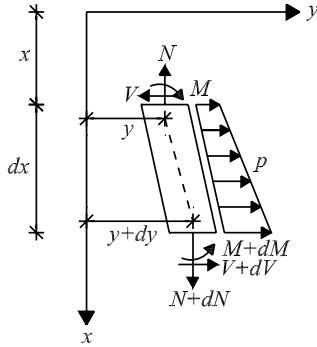


**Figure 4:** Sign convention for infinitesimal beam element.

With use of (2)–(4) and the kinematic assumption  $\kappa = \frac{d^2y}{dx^2}$  which is assumed in Bernoulli-Euler beam theory the governing fourth-order differential equation for determination of deflection is obtained:

$$E_p I_p \frac{d^4y}{dx^4} - N \frac{d^2y}{dx^2} + E_{py}y = 0 \quad (5)$$

In (5) the shear strain,  $\gamma$ , in the beam is neglected. This assumption is only valid for relatively slender beams. For short and rigid beams the Timoshenko beam theory, that takes the shear strain into account,

is preferable. The following relations are used:

$$V = G_p A_v \gamma \quad (6)$$

$$\gamma = \frac{dy}{dx} - \omega \quad (7)$$

$$\kappa = \frac{d\omega}{dx} \quad (8)$$

$G_p$  and  $A_v$  are the shear modulus and the effective shear area of the beam, respectively.  $\omega$  is the cross-sectional rotation as defined in fig. 5. In Timoshenko beam theory the shear strain and hereby the shear stress is assumed to be constant over the cross section. However, in reality the shear stress varies parabolic over the cross section. The effective shear area is defined so the two stress variations give the same shear force. For a pipe the effective shear area can be calculated as:

$$A_v = 2(D - t)t \quad (9)$$

where  $t$  is the wall thickness of the pipe.

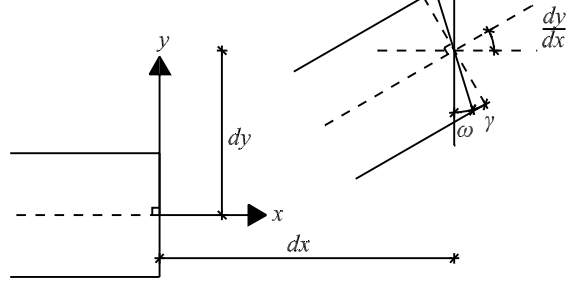


**Figure 5:** Shear and curvature deformation of a beam element.

By combining (1)–(4) and (6)–(8) two coupled differential equations can be formulated to describe the deflection of the Timoshenko beam:

$$G A_v \frac{d}{dx} \left( \frac{dy}{dx} - \omega \right) - E_{py}y = 0 \quad (10)$$

$$E_p I_p \frac{d^3\omega}{dx^3} - N \frac{d^2y}{dx^2} + E_{py}y = 0 \quad (11)$$

In the derivation of the differential equations the following assumptions have been used:

- The beam is straight and has a uniform cross section.
- The beam has a longitudinal plane of symmetry, in which loads and reactions lie.
- The beam material is homogeneous, isotropic, and elastic. Furthermore, plastic hinges do not occur in the beam.
- Young's modulus of elasticity of the beam material is similar in tension and compression.
- Beam deflections are small.
- The beam is not subjected to dynamic loading.

### 3 Formulations of $p$ - $y$ curves for piles in sand

$p$ - $y$  curves describing the static and cyclic behaviour of piles in cohesionless soils are presented followed by a discussion of their validity and limitations, cf. section 4. Only the formulation made by Reese et al. (1974), hereafter denoted Method A, and the formulation proposed by O'Neill and Murchison (1983) and implemented in design regulations such as API (2000) and DNV (2010), Method B, will be described. Both  $p$ - $y$  curve formulations are empirically derived based on full-scale tests on free-ended piles at Mustang Island.

#### 3.1 Full-scale tests at Mustang Island

Tests on two fully instrumented, identical piles located at Mustang Island, Texas as described by Cox et al. (1974), are the starting point for the formulation of  $p$ - $y$  curves for piles in sand. The test setup is shown in fig. 6 and 7.

To install the test- and reaction piles a Delmag-12 diesel hammer was used. The test piles were steel pipe piles with diameters of  $D = 0.61$  m (24 in) and wall thicknesses of  $wt = 9.5$  mm (3/8 in). The embedded length of the piles were 21.0 m (69 ft) which corresponds to a slenderness ratio of  $L/D = 34.4$ . The piles were instrumented with a total of 34 active strain gauges mounted from 0.3 m above the mudline to 9.5 m (32 ft) below the mudline. The strain gauges were bonded directly to the inside of the pile in 17 levels with highest concentration of gauges near the mudline. The horizontal distance between the centre of the two test piles was 7.5 m (24 ft and 8 in), cf. fig. 7. Between the piles the load cell was installed on four reaction piles. The minimum horizontal distance from the centre of a reaction pile to the centre of a test pile was 2.8 m (9 ft and 4 in). Hence, from each test pile, two reaction piles were placed each with an angle of approximately  $28^\circ$  from the direction of loading. Hence, the total center to center distance from each test pile to the nearest reaction piles were 3.2 m corresponding to  $5.2D$ . According to Remaud et al. (1998), a trailing pile positioned respectively  $4D$  and  $6D$  away from the leading pile has in general a reduction in stiffness and capacity of 18 and 7 %, respectively. Therefore, a minor effect from the reaction piles must be expected. Neither Cox et al. (1974) nor Reese et al. (1974) mentions whether they account for group effects in the analysis of the pile tests.

Prior to pile installation, two soil borings were made, each in a range of 3.0 m (10 ft) from a test pile. The soil samples showed a slight difference between the two areas where the piles were installed, as one boring contained fine sand in the top 12 m (40 ft) and the other contained silty fine sand. The strength parameters were derived from standard penetration tests according to Peck et al. (1953). The standard penetration tests showed large variations in the number of blows per ft. Espe-

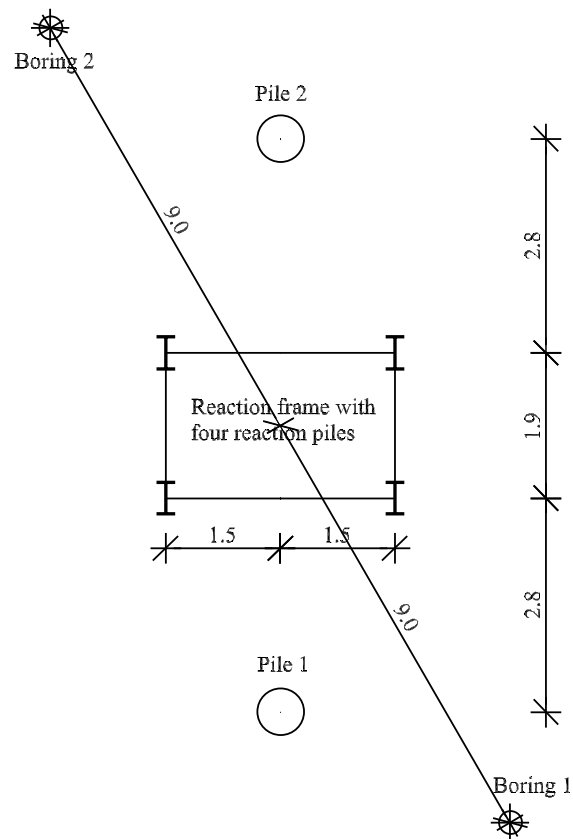


**Figure 6:** Plan drawing of the test setup for the Mustang Island tests, after Cox et al. (1974). Measures in meter.

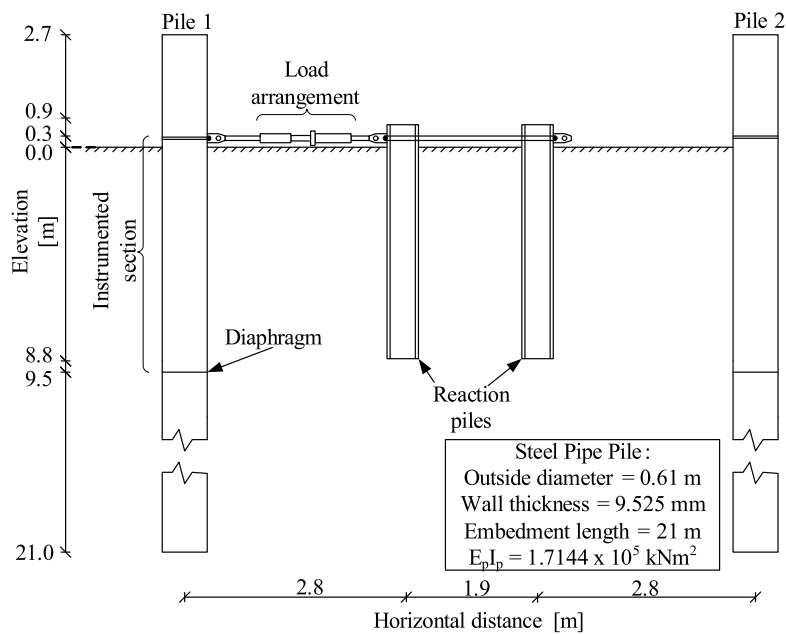


**Figure 7:** Cross-sectional view of the test setup for the Mustang Island tests, after Cox et al. (1974).

cially in the top 12 m (40 ft) of both borings the number of blows per 30 cm varied from 10 to 80. From 12 to 15 m (40 to 50 ft) beneath the mudline clay was encountered. Beneath the clay layer the strength increased from 40 to 110 blows per 30 cm. From 18 m (60 ft) beneath the mudline to the total depth the number of blows per 30 cm decreased from 110 to 15. The water table was located at the soil surface, implying fully saturated soil.

The piles were in total subjected to seven horizontal load cases consisting of two static and five cyclic. Pile 1 was at first subjected to a static load test 16 days after installation. The load was applied in increments until a maximum load of 267 kN (60000 lb) was reached. The maximum load was determined as no failure occurred in the pile. After the static load test on pile 1 two cyclic load tests were conducted with varying load amplitude. A maximum of 25 load cycles were applied. 52 days after installation a pull-out test was conducted on pile 2. A maximum of 1780 kN (400000 lb) was applied causing the pile to move 25 mm (1 inch). After another week pile 2 was subjected to three cases of cyclic loading and finally a static load test. For the cyclic loading a maximum of 100 load cycles were applied. The static load case on pile 2 was performed immediately after the third cyclic load case which might affect the results. Reese et al. (1974) do not clarify whether this effect is considered in the analyses.

### 3.2 Method A

Method A is the original method based on the Mustang Island tests, cf. Reese et al. (1974). The  $p$ - $y$  curve formulation consists of three curves: an initial straight line,  $p_1$ , a parabola,  $p_2$ , and a straight line,  $p_3$ , all assembled to one continuous piecewise differentiable curve, cf. fig. 8. The last straight line from  $(y_m, p_m)$  to  $(y_u, p_u)$

is bounded by an upper limit characterised by the ultimate soil resistance,  $p_u$ .

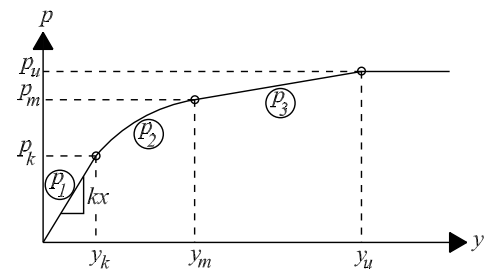


**Figure 8:**  $p$ - $y$  curve for static loading using method A, after Reese et al. (1974).

### Ultimate soil resistance

The total ultimate lateral resistance,  $F_{pt}$ , is equal to the passive force,  $F_p$ , minus the active force,  $F_a$ , acting on the pile. The ultimate resistance can be estimated analytically by means of either statically or kinematically admissible failure modes. At shallow depths a wedge will form in front of the pile assuming that the Mohr-Coulomb failure criterion is valid. Reese et al. (1974) uses the wedge shown in fig. 9 to analytically calculate the passive ultimate resistance at shallow depths,  $p_{cs}$ . By using this failure mode a smooth pile is assumed, and therefore no tangential forces occur at the pile surface. The active force is also computed from Rankine's failure mode, using the minimum coefficient of active earth pressure.

At deep depths the sand will, in contrast to shallow depths, flow around the pile and a static failure mode as sketched in fig. 10 is used to calculate the ultimate resistance. The transition depth between these failure modes occurs, at the depth where the ultimate resistances calculated based on the two failure modes are identical.

The ultimate resistance per unit length of the pile can for the two failure modes be

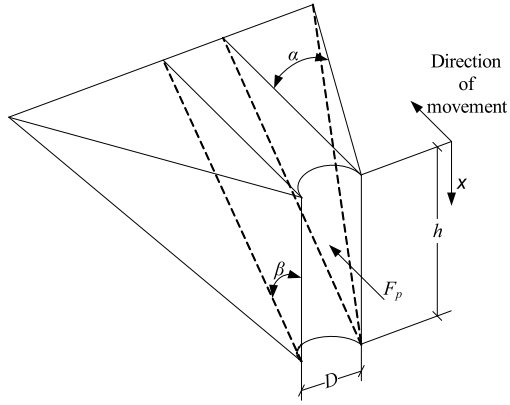


**Figure 9:** Failure mode at shallow depths, after Reese et al. (1974).

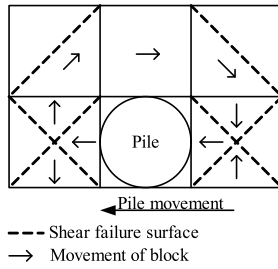


**Figure 10:** Failure mode at deep depths, after Reese et al. (1974).

calculated according to (12) and (13):

$$p_{cs} = \gamma' x \frac{K_0 x \tan \varphi_{tr} \sin \beta}{\tan(\beta - \varphi_{tr}) \cos \alpha} \quad (12)$$

$$+ \gamma' x \frac{\tan \beta}{\tan(\beta - \varphi_{tr})} (D - x \tan \beta \tan \alpha) \\ + \gamma' x (K_0 x \tan \varphi_{tr} (\tan \varphi_{tr} \sin \beta - \tan \alpha) - K_a D)$$

$$p_{cd} = K_a D \gamma' x (\tan^8 \beta - 1) \quad (13) \\ + K_0 D \gamma' x \tan \varphi_{tr} \tan^4 \beta$$

$p_{cs}$  is valid at shallow depths and  $p_{cd}$  at deep depths,  $\gamma'$  is the effective unit weight, and  $\varphi_{tr}$  is the angle of internal friction based on triaxial tests. The factors  $\alpha$  and  $\beta$  measured in degrees can be estimated by the following relations:

$$\alpha = \frac{\varphi_{tr}}{2} \quad (14)$$

$$\beta = 45^\circ + \frac{\varphi_{tr}}{2} \quad (15)$$

Hence, the angle  $\beta$  is estimated according to Rankine's theory which is valid if the

pile surface is assumed smooth. The factor  $\alpha$  depends on the friction angle and load type. However, the effect of load type is neglected in (14).  $K_a$  and  $K_0$  are the coefficients of active horizontal earth pressure and horizontal earth pressure at rest, respectively:

$$K_a = \tan^2(45 - \frac{\varphi_{tr}}{2}) \quad (16)$$

$$K_0 = 0.4 \quad (17)$$

The value of  $K_0$  depends on several factors, e.g. the friction angle, but (17) does not reflect that.

The theoretical ultimate resistance,  $p_c$ , as function of depth is shown in fig. 11. As shown, the transition depth increases with diameter and angle of internal friction. Hence, for piles with a low slenderness ratio the transition depth might appear far beneath the pile-toe.

By comparing the theoretical ultimate resistance,  $p_c$ , with the full-scale tests at Mustang Island, Cox et al. (1974) found a poor agreement. Therefore, a coefficient  $A$  is introduced when calculating the actual ultimate soil resistance,  $p_u$ , employed in the  $p$ - $y$  curve formulations:

$$p_u = A p_c \quad (18)$$

The variation of the coefficient  $A$  with non-dimensional depth,  $x/D$ , depends on whether static or cyclic loading is applied. The variation of  $A$  is shown in fig. 12a. The deformation causing the ultimate soil resistance,  $y_u$ , cf. fig. 8, is defined as  $3D/80$ .

### $p$ - $y$ curve formulation

The soil resistance per unit length,  $p_m$ , at  $y_m = D/60$ , cf. fig. 8, can be calculated as:

$$p_m = B p_c \quad (19)$$

$B$  is a coefficient depending on the non-dimensional depth  $x/D$ , and whether static or cyclic loading is considered. The variation of  $B$  with non-dimensional depth is

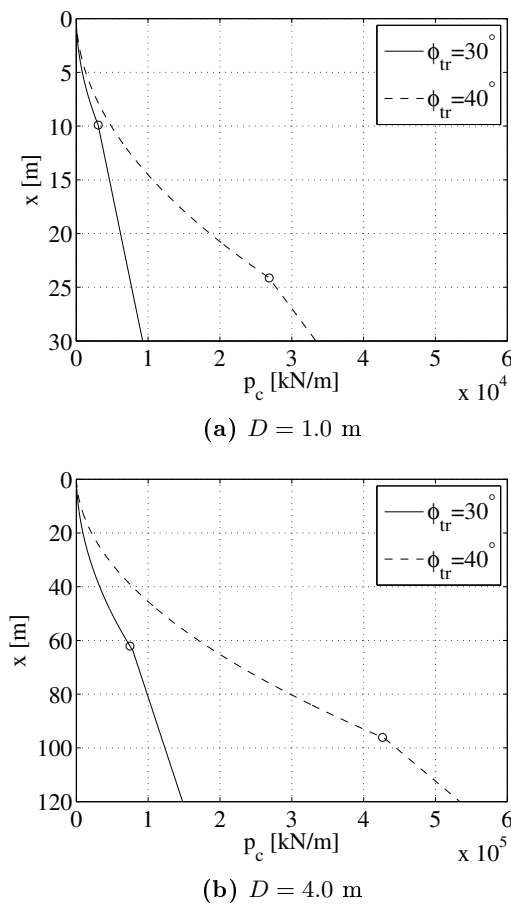
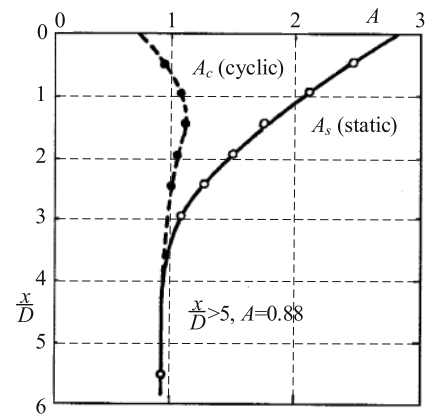


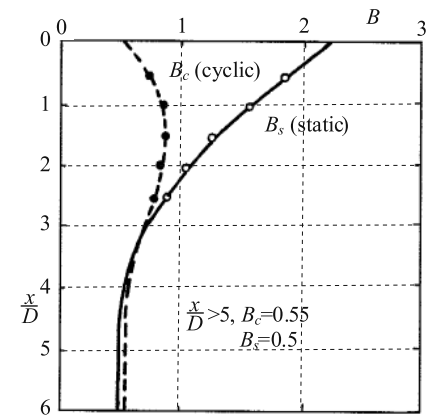
**Figure 11:** Theoretical ultimate resistance,  $p_c$ , as function of the depth.  $\gamma' = 10 \text{ kN/m}^3$  has been used to plot the figure. The transition depths are marked with circles.

illustrated in fig. 12b. Hence, cyclic loading is taken into account by a reduction of the non-dimensional constants  $A$  and  $B$ . Cyclic loading only affects the  $p$ - $y$  curves significantly at depths from the soil surface to  $x/D = 3.5$ .

The slope of the initial straight line,  $p_1$  as shown in fig. 8, depends on the initial modulus of subgrade reaction,  $k$ , and the depth  $x$ . This is due to the fact that the in-situ Young's modulus of elasticity also increases with depth. Further, it is assumed that the slope of the initial straight line increases linearly with depth since laboratory test shows, that the initial slope of the stress-strain curve for sand is a linear function of the confining pressure, cf. Terzaghi (1955). The initial tangent stiffness of the



**(a)** Non-dimensional coefficient  $A$  for determining the ultimate soil resistance,  $p_u$ .



**(b)** Non-dimensional coefficient  $B$  for determining the soil resistance,  $p_m$ .

**Figure 12:** Non-dimensional variation of  $A$  and  $B$ , after Reese et al. (1974).

$p$ - $y$  curves is in the following denoted  $E_{py}^*$ . The initial straight line is given by:

$$p_1(y) = E_{py}^* y = kxy \quad (20)$$

Reese et al. (1974) suggest that the value of  $k$  only depends on the relative density/internal friction angle for the sand. On basis of full-scale experiments values of  $k$  for loose sands, for medium dense sands, and for dense sands are  $5.4 \text{ MN/m}^3$  ( $20 \text{ lbs/in}^3$ ),  $16.3 \text{ MN/m}^3$  ( $60 \text{ lbs/in}^3$ ), and  $34 \text{ MN/m}^3$  ( $125 \text{ lbs/in}^3$ ), respectively. The values are valid for sands below the water table. Earlier estimations of  $k$  has also been made, for example by Terzaghi (1955), but according to Reese and Van Impe (2001) these methods have been



based on intuition and insight. Design regulations, e.g. API (2000) and DNV (2010), recommend the use of the curve shown in fig. 13. The curve only shows data for relative densities up to approximately 80 %, which causes large uncertainties in the estimation of  $k$  for very dense sands.

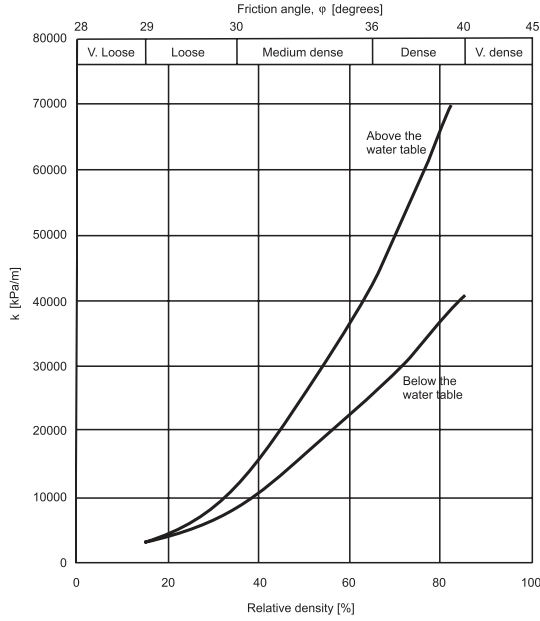


**Figure 13:** Variation of initial modulus of sub-grade reaction  $k$  as function of relative density, after API (2000).

The equation for the parabola,  $p_2$ , cf. fig. 8, is described by:

$$p_2(y) = Cy^{1/n} \quad (21)$$

where  $C$  and  $n$  are constants. The constants and the parabola's start point  $(y_k, p_k)$  are determined by the following criteria:

$$p_1(y_k) = p_2(y_k) \quad (22)$$

$$p_2(y_m) = p_3(y_m) \quad (23)$$

$$\frac{\partial p_2(y_m)}{\partial y} = \frac{\partial p_3(y_m)}{\partial y} \quad (24)$$

The constants can then be calculated by:

$$n = \frac{p_m}{my_m} \quad (25)$$

$$C = \frac{p_m}{y_m^{1/n}} \quad (26)$$

$$y_k = \left(\frac{C}{kx}\right)^{n/(n-1)} \quad (27)$$

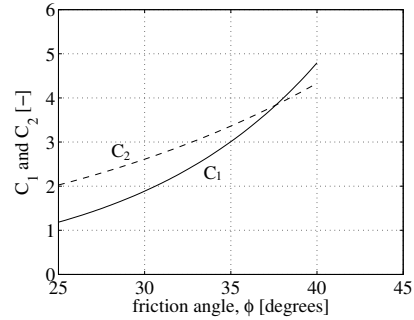
where  $m$  is the slope of the line,  $p_3$ .

### 3.3 Method B

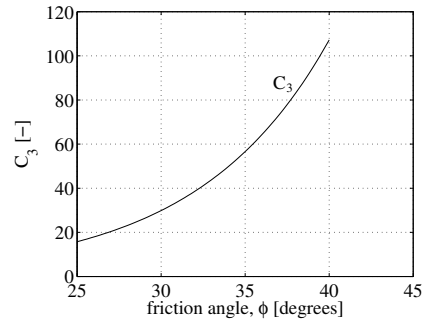
O'Neill and Murchison suggested a modified formulation of the  $p$ - $y$  curves. The modified expression is currently recommended in the design regulations, e.g. API (2000) and DNV (2010). In their modified  $p$ - $y$  curve formulation, the analytical expressions for the ultimate soil resistance, (12) and (13), are approximated using the dimensionless parameters  $C_1$ ,  $C_2$  and  $C_3$ :

$$p_u = \min \left( \begin{array}{l} p_{us} = (C_1x + C_2D)\sigma'_v \\ p_{ud} = C_3D\sigma'_v \end{array} \right) \quad (28)$$

The constants  $C_1$ ,  $C_2$  and  $C_3$  can be determined from fig. 14.



(a)  $C_1$  and  $C_2$ .



(b)  $C_3$ .

**Figure 14:** Variation of the parameters  $C_1$ ,  $C_2$  and  $C_3$  as function of angle of internal friction, after API (2000).

A hyperbolic formula is used to describe the relationship between soil resistance and pile deflection instead of a piecewise formulation as proposed by method A:

$$p(y) = Ap_u \tanh \left( \frac{kx}{Ap_u} y \right) \quad (29)$$

The coefficient  $A$  could either be determined from fig. 12a or by:

$$A = \begin{cases} 3.0 - 0.8\frac{H}{D} \geq 0.9, & \text{static loading} \\ 0.9 & \text{cyclic loading} \end{cases} \quad (30)$$

Since:

$$\frac{dp}{dy} \Big|_{y=0} = Ap_u \frac{\frac{kx}{Ap_u}}{\cosh^2\left(\frac{kxy}{Ap_u}\right)} \Big|_{y=0} = kx \quad (31)$$

the  $p$ - $y$  curve's initial slope is then similar using the two methods, cf. (20). Also the upper bound of soil resistance will approximately be the same. However, there is a considerable difference in soil resistance predicted by the two methods when considering the pile deflection between  $y_k$  and  $y_u$  as shown in fig. 15. The soil parameters from tab. 1 has been used to construct the  $p$ - $y$  curves shown in fig. 15.

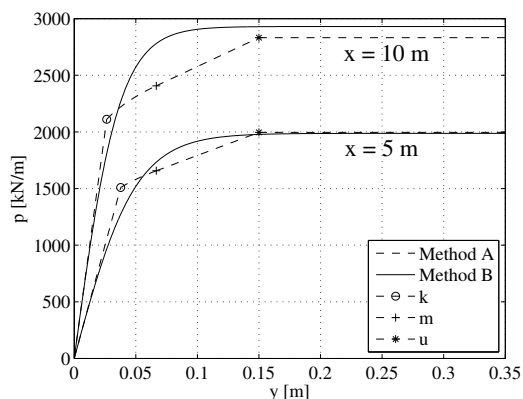


**Figure 15:** Example of  $p$ - $y$  curves based on method A and B. The points  $k$ ,  $m$ , and  $u$  refers to the points  $(y_k, p_k)$ ,  $(y_m, p_m)$ , and  $(y_u, p_u)$ , respectively, cf. fig. 8.

**Table 1:** Soil parameters used for plotting the  $p$ - $y$  curves in fig. 15.

$\gamma'$	$\phi_{tr}$	$D$	$k$
[kN/m <sup>3</sup> ]	[°]	[m]	[kN/m <sup>3</sup> ]
10	30	4.2	8000

### 3.4 Comparison of methods

A comparison of both static and cyclic  $p$ - $y$  curves has been made by Murchison and

O'Neill (1984) based on a database of 14 full-scale tests on 10 different sites. The pile diameters varied from 51 mm (2 in.) to 1.22 m (48 in.). Both timber, concrete and steel piles were considered. The soil friction angles ranged from 23° to 42°. The test piles' slenderness ratio's are not provided.

Murchison and O'Neill (1984) compared the  $p$ - $y$  curve formulations formulated by Reese et al. (1974), Bogard and Matlock (1980), Scott (1980), and O'Neill and Murchison (1983) with the full-scale tests using the Winkler approach. The predicted pile-head deflection, maximum moment,  $M_{max}$ , and the depth of maximum moment were compared according to the error,  $E$ :

$$E = \frac{|\text{predicted value} - \text{measured value}|}{\text{measured value}} \quad (32)$$

In the analysis it was desired to assess the formulations ability to predict the behaviour of steel pipe monopiles. Multiplication factors were therefore employed. The error,  $E$ , was multiplied by a factor of two for pipe piles, 1.5 for non-pipe driven piles and a factor of one for drilled piers. When predicted values were lower than the measured values the error was multiplied by a factor of two. By using these factors unconservative results are penalised and pipe piles are valued higher in the comparison. In tab. 2 the average value of  $E$  for static  $p$ - $y$  curves are shown for the four methods, and in tab. 3 the average value of  $E$  is shown for the cyclic  $p$ - $y$  curves. As shown, the formulation proposed by O'Neill and Murchison (1983), cf. method B, results in a lower average value of  $E$ . The standard deviation of  $E$  was not provided in the comparison.

In their comparison of the four  $p$ - $y$  curve formulations with the database of tests, Murchison and O'Neill (1984) observed that method A often predicted larger displacement than what was measured. Hence, method A seems to be conserva-

**Table 2:** Average values of the error,  $E$ , for the static pile tests. The methods are compared for pile-head deflection, maximum moment and depth to maximum moment.

	Pile-head deflection	$M_{\max}$	Depth to $M_{\max}$
Reese et al. (1974)	2.08	0.75	0.58
Bogard and Matlock (1980)	1.95	0.73	0.52
Scott (1980)	2.31	0.58	0.37
O'Neill and Murchison (1983)	1.44	0.44	0.40

**Table 3:** Average values of the error,  $E$ , for the cyclic pile tests. The methods are compared for pile-head deflection, maximum moment and depth to maximum moment.

	Pile-head deflection	$M_{\max}$	Depth to $M_{\max}$
Reese et al. (1974)	1.15	0.61	0.16
Bogard and Matlock (1980)	1.22	0.55	0.12
O'Neill and Murchison (1983)	0.55	0.5	0.16

tive. In contrast method B were neither found to be conservative nor unconservative.

Murchison and O'Neill (1984) analysed the sensitivity to parameter variation for method B. The initial modulus of subgrade reaction,  $k$ , the internal friction angle,  $\varphi$ , and the effective unit weight,  $\gamma'$ , were varied. They found that a 10 % increase in either  $\varphi$  or  $\gamma'$  resulted in an increase in pile-head deflection of up to 15 and 10 %, respectively. For an increase of 25 % in  $k$  an increase of up to 10 % of the pile-head deflection was found. The sensitivity analysis also shows that  $k$  has the greatest influence on pile-head deflection at small deflections and that  $\varphi$  has a great

influence at large deflections. Murchison and O'Neill (1984) state that the sizes of the errors in tab. 2 cannot be explained by parameter uncertainties. The amount of data included in the database was very small due to the unavailability of appropriately documented full-scale tests and Murchison and O'Neill (1984) therefore concluded that a further study of the soil-pile interaction was needed.

## 4 Limitations of $p$ - $y$ curves

The  $p$ - $y$  curve formulations for piles in cohesionless soils are developed for piles with diameters much less than 4 to 6 m which is often necessary for nowadays monopiles. Today, there is no approved method for dealing with these large-diameter, non-slender offshore piles, which is why the design regulations are still adopting the original  $p$ - $y$  curve formulations (Reese et al., 1974; O'Neill and Murchison, 1983; API, 2000; and DNV, 2010).

The  $p$ - $y$  curve formulations are derived on the basis of the Mustang Island tests which included only two identical piles and a total of seven load cases. Furthermore, the tests were conducted for only one pile diameter, one type of sand, only circular pipe piles, etc. Taking into account the number of factors that might affect the behaviour of a laterally loaded pile and the very limited number of full-scale tests performed to validate the method, the influence of a broad spectra of parameters in the  $p$ - $y$  curves are still to be clarified. When considering offshore wind turbine foundations a validation of stiff piles with a slenderness ratio of  $L/D < 10$  is needed. It is desirable to investigate this as it might have a significant effect on the initial stiffness which is not accounted for in the  $p$ - $y$  curve method. Briaud et al. (1984) postulate that the soil response depends on the flexibility of the pile. Criteria for stiff versus flexible behaviour of piles have been

proposed by various authors, for example, Dobry et al. (1982), Budhu and Davies (1987), and Poulos and Hull (1989). The difference in deformation behaviour of a stiff and a flexible pile is shown in fig. 16. A pile behaves rigidly when the following criterion is fulfilled (Poulos and Hull, 1989):

$$L < 1.48 \left( \frac{E_p I_p}{E_s} \right)^{0.25} \quad (33)$$

$E_s$  is Young's modulus of elasticity of the soil. The criterion for flexible pile behaviour is (Poulos and Hull, 1989):

$$L > 4.44 \left( \frac{E_p I_p}{E_s} \right)^{0.25} \quad (34)$$

According to (33) a monopile with an outer diameter of 4 m, an embedded length of 20 m and a wall thickness of 0.05 m behaves rigidly if  $E_s < 7.6$  MPa. In contrast, the pile exhibits a flexible behaviour if  $E_s > 617$  MPa. Even dense sands have  $E_s < 100$  MPa, so the recently installed monopiles for offshore wind turbines behave, more like rigid than flexible piles.

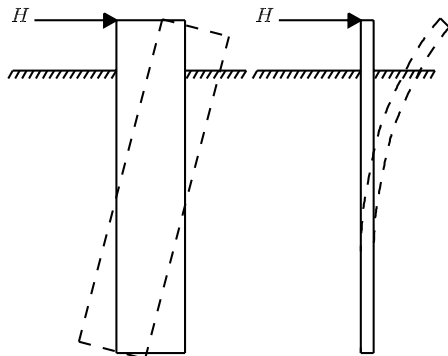


**Figure 16:** Rigid versus flexible pile behaviour.

The current expression for the ultimate soil resistance is an analytical expression derived for a lateral pile translation. A correction factor for the ultimate soil resistance based on full-scale tests on flexible piles is employed. However, as monopiles for offshore wind turbines behave more rigidly than flexibly the combination of the analytical expression and the correction factor might be a poor approximation of

the ultimate soil resistance for rigid piles. Hence, the ultimate soil resistance needs validation for large-diameter, non-slender piles.

Only small pile-head rotations are acceptable for modern wind turbine foundations. The allowable pile rotation is provided by the wind turbine supplier. Typically  $0.5^\circ$  of accumulated plastic pile rotation is acceptable. Furthermore, it is of high importance to avoid resonance of the wind turbine with the blade frequency, the rotor frequency and the energy rich frequency of the loading. Hence, it is important to model the foundation stiffness correctly. Appropriate values for the initial stiffness of the  $p$ - $y$  curves are therefore necessary.

When using the  $p$ - $y$  curve method, the pile bending stiffness is employed when solving the beam on an elastic foundation problem. However, no importance is given to the pile bending stiffness in the formulation of the  $p$ - $y$  curves. Hence,  $E_{py}$  is independent of the pile properties. The validity of this assumption can be questioned as  $E_{py}$  is a parameter describing the soil-pile interaction.

When decoupling the non-linear springs associated with the Winkler model approach another error is introduced, since the soil in reality acts as a continuum.

The design regulations suggests the use of a tangent hyperbolic  $p$ - $y$  curve, cf. (29). The reason for this is based on the comparison reported by Murchison and O'Neill (1984) of four different  $p$ - $y$  curve formulations. When using this approach, the initial slope of the  $p$ - $y$  curves and the ultimate soil resistance governs the shape of the curve. However, the validity of the tangent hyperbolic formulation can be questioned.

The  $p$ - $y$  curve formulation is based on full-scale tests on piles installed in rather homogeneous soil. However, often piles are to be installed in a strongly layered strat-

ification. The effect of layered soil on the soil-pile interaction therefore needs to be investigated.

Offshore wind turbines are exposed to cyclic loading from wind and waves. During the lifetime of an offshore wind turbine (typically 20 years) the foundation will be exposed to few load cycles of high load amplitude and  $10^6 - 10^8$  load cycles of low to intermediate load amplitude. The  $p-y$  curve formulations proposed by Reese et al. (1974) and O'Neill and Murchison (1983) are based on full-scale tests on piles for the oil and gas sector. In these full-scale tests, the pile behaviour for cyclic loading with up to 100 load cycles was investigated. Hence, the behaviour of the piles with respect to long-term cyclic loading were not investigated. The accumulated pile deflection and the change in pile stiffness due to long-term cyclic loading therefore needs to be addressed.

Around pile foundations in the offshore environment, erosion of soil material can occur due to turbulence. Scour holes will therefore form around the pile foundations. Scour is especially an issue for cohesionless soil materials. Scour holes can when they are fully developed be up to  $1.3D$  (DNV, 2010). When a scour hole has been formed, soil support is lost. Hence, the  $p-y$  curves needs modification to account for scour.

In the following a number of assumptions and not clarified parameters related to the  $p-y$  curve method are treated separately. The treated assumptions and parameters are:

- Shearing force between soil layers.
- The ultimate soil resistance.
- The influence of vertical pile load on lateral soil response.
- Effect of soil-pile interaction.

- Effect of diameter on initial stiffness of  $p-y$  curves.
- Choice of horizontal earth pressure coefficient.
- Shearing force at the pile-toe.
- Shape of  $p-y$  curves.
- Layered soil.
- Long-term cyclic loading.
- Scour effect on the soil-pile interaction.

#### 4.1 Shearing force between soil layers

Employing the Winkler model approach, the soil response is divided into layers each represented by non-linear springs. As the springs are uncoupled, the layers are considered to be independent of the lateral pile deflection above and below that specific layer, giving that the soil layers are considered as smooth layers able to move relatively to each other without loss of energy to friction. Pasternak (1954) modified the Winkler approach by taking the shear stress between soil layers into account. The soil resistance per length of the pile is given by:

$$p(y) = -E_{py}^p y - G_s \frac{dy}{dx} \quad (35)$$

where  $G_s$  is the soil shear modulus. The traditional subgrade reaction modulus,  $E_{py} = p/y$ , may indirectly contain the soil shear stiffness as the  $p-y$  curve formulation has been fitted to full-scale tests.  $E_{py}^p$ , cf. (35), is a modulus of subgrade reaction without contribution from the soil shear stiffness.

Belkhir et al. (1999) examines the significance of shear between soil layers by comparing the CAPELA design code, which can take the shear between soil layers into account, with the French PILATE design

code, which employs smooth boundaries. The two design codes are compared with the results of 59 centrifuge tests conducted on long and flexible piles. Analyses show concordance between the two design codes when shear between soil layers is not taken into account. Furthermore, the analyses shows a reduction varying from 5 % to 14 % in the difference between the maximum moments determined from the centrifuge tests and the numerical simulations when taking the shear between the soil layers into account. However, it is not clear from the paper whether or not the shear between soil layers is dependent on pile properties such as pile diameter, slenderness ratio, etc. Furthermore, it is not clarified whether the authors distinguish between  $E_{py}$  and  $E_{py}^p$ .

## 4.2 The ultimate soil resistance

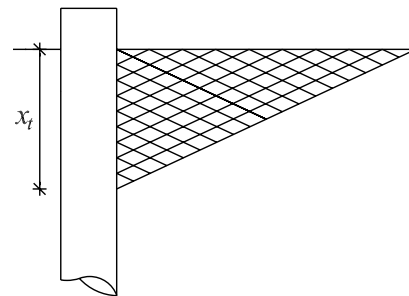
The  $p$ - $y$  curve formulations according to Method A and Method B are both dependent on the ultimate soil resistance. The method for estimation of  $p_u$  is therefore evaluated in the following.

### Failure modes

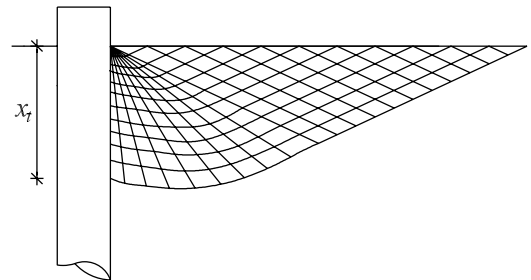
When designing large-diameter monopiles in sand, the transition between the presumed failure modes will most often occur beneath the pile-toe, cf. fig. 11b. Therefore, the ultimate soil resistance at shallow depths is governing for monopile foundations for offshore wind turbines. However, several uncertainties concerning the expression for the ultimate soil resistance at shallow depths exist.

The prescribed method for calculating the ultimate soil resistance at shallow depths assumes that the pile is smooth, which means that no skin friction appears between the pile wall and the soil, and further the formation of a Rankine failure is assumed. However, in reality a pile

is neither perfectly rough nor perfectly smooth, and the assumed failure mechanism is therefore not correct. According to Harremoës et al. (1984) a Rankine failure takes place for a perfectly smooth wall and a Prandtl failure for a perfectly rough wall. Sketches of the two types of failure are shown in fig. 17a and fig. 17b, respectively. Due to the fact that the pile is neither smooth nor rough a combination of a Rankine and Prandtl failure will occur.



(a) Failure mode proposed by Rankine for a smooth interface at shallow depth.



(b) Failure mode proposed by Prandtl for a rough interface at shallow depth.

**Figure 17:** Rankine and Prandtl failure modes.

In (12) the angle  $\alpha$ , which determines the horizontal spread of the wedge, appears. Through experiments Reese et al. (1974) postulate that  $\alpha$  depends on both the void ratio, the friction angle, and the type of loading. However, the influence of void ratio and type of loading is neglected in the expression of  $\alpha$ , cf. (14).

Monopiles for offshore wind turbines are non-slender piles with high bending stiffness. The piles therefore deflect as almost rigid piles. As the piles are exposed to eccentric loading, the pile deformation pattern primarily consists of rotation around

a point of zero deflection. Hence, the pile deflection at the pile toe is negative. However, when calculating the ultimate soil resistance according to method A and B the rotational pile behaviour and hereby negative pile deflections beneath the point of zero deflection is disregarded. For non-slender piles, a failure mode as shown in fig. 18 could potentially form. This failure mode is derived for a two-dimensional case assuming a smooth pile surface. The failure mode consists of stiff elastic zones and Rankine failures.

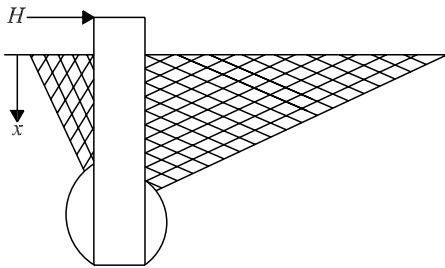


**Figure 18:** Possible failure mode for a non-slender pile at shallow depth, after Harremoës et al. (1984).

### Soil dilatancy

The effect of soil dilatancy is not included in method A and B, and thereby the effects of volume changes during pile deflection are ignored.

Fan and Long (2005) investigated the influence of soil dilatancy on the ultimate soil resistance by use of a three-dimensional, non-linear finite element model. The constitutive model proposed by Desai et al. (1991) incorporating a non-associative flow rule was employed in the analyses. The finite element model was calibrated based on the full-scale tests at Mustang Island. The magnitudes of ultimate soil resistance were calculated for two compactions of one sandtype with similar friction angles ( $\varphi_{tr} = 45^\circ$ ) but different angles of dilatancy. The dilatancy angles are not directly specified by Fan and Long (2005). Estimates have therefore

been made by interpretation of the relation between volumetric strains and axial strains. Dilatancy angles of approximately  $22^\circ$  and  $29^\circ$  were found. An increase in ultimate soil resistance of approximately 50 % were found with the increase in dilatancy angle. In agreement with laboratory tests, where the dilatancy in dense sands contributes to strength, this makes good sense. It should be noted that the dilatancy angle and the soil friction angle are related such that soil materials with a high value for the friction angle typically also has a high value for the dilatancy angle. Hence, the effect of soil dilatancy might be implicitly incorporated in the expression for the ultimate resistance and the correction factor  $A$ . Further, it should be noted that accurate determination of the dilatancy angles requires expensive soil tests, for example, triaxial tests.

### Alternative methods

Besides the prescribed method for calculating the ultimate soil resistance several other formulations exist (e.g. Hansen, 1961; Broms, 1964; Petrasovits and Award, 1972; Meyerhof et al., 1981; and Prasad and Chari, 1999). Fan and Long (2005) compared the methods of Hansen (1961) and Broms (1964) with method B and a finite element solution. In the comparison, the pile diameter, the friction angle, and the coefficient of horizontal earth pressure were varied. Hansen's method showed the best correlation with the finite element model, whereas Broms' method resulted in conservative values of the ultimate soil resistance. Further, a significant difference between the finite element solution and method B was found. Method B was found to produce conservative results at shallow depths and non-conservative results at deep depths. The results of the comparison are shown in fig. 19.

The expression of the ultimate soil resistance formulated by Hansen (1961),

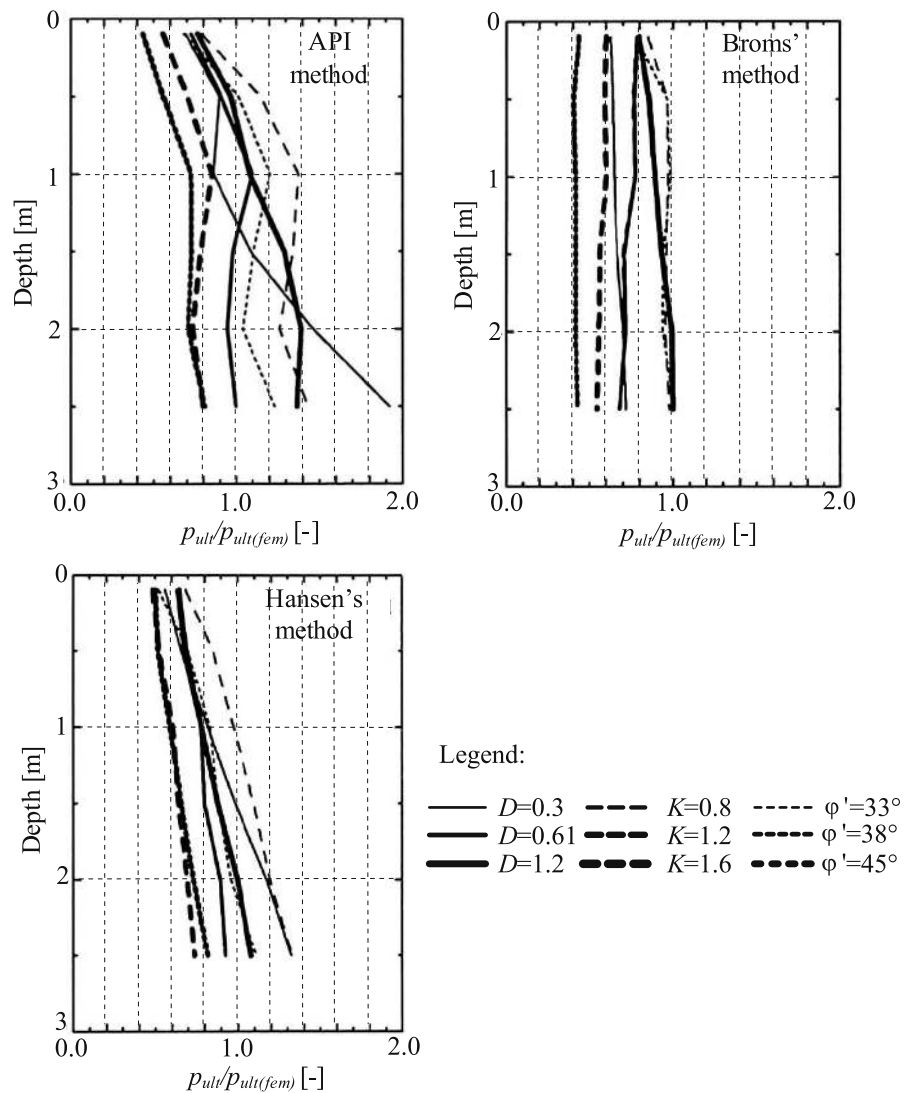


**Figure 19:** Comparison of the ultimate soil resistance estimated by Broms' method, Hansen's method, and method B with a finite element model, after Fan and Long (2005).  $p_{ult}/p_{ult(fem)}$  defines the ratio of the ultimate soil resistance calculated by the analytical methods and the ultimate soil resistance calculated by the finite element model.

Broms (1964), Petrasovits and Award (1972), Meyerhof et al. (1981), and Reese et al. (1974) all assumes the soil pressure to vary uniformly with the pile width. Prasad and Chari (1999) formulated an expression based on small-scale tests on rigid piles instrumented with pressure transducers. They measured the variation of soil pressure with depth and horizontal position on the pile. The test piles had diameters of 0.102 m and slenderness ratios of 3-6. They determined failure as the point in which the load-displacement curves started to be linear. Hence, a hor-

izontal asymptote was not reached and it can be argued whether or not their definition of failure is reasonable. Various researchers have expressed criteria for pile failure, for instance, LeBlanc et al. (2010). They considered a horizontally loaded pile to be in failure when the normalised pile rotation,  $\bar{\Theta}$ , exceeds  $4^\circ$ . They defined the normalised pile rotation as:

$$\bar{\Theta} = \Theta \sqrt{\frac{p_a}{\gamma' L}} \quad (36)$$

Failure was by Prasad and Chari (1999) found at pile displacements of  $0.2-0.4D$ .



Based on the load tests on rigid piles, they formulated a new expression for the ultimate soil resistance for laterally loaded rigid piles in which the ultimate soil resistance depends on parameters such as the friction angle, the pile diameter, the pile length and the depth of the point of zero pile deflection. Their expression consists of three linear curves describing the variation of the ultimate soil resistance with depth. The expressions of Hansen (1961), Broms (1964), Petrasovits and Award (1972), Meyerhof et al. (1981) and Prasad and Chari (1999) are sketched in fig. 20. All except Prasad and Chari (1999) postulate that the ultimate resistance at the depth of zero pile deflection is non-zero.

When calculating the ultimate soil resistance according to method A and B, the side friction as illustrated in fig. 21 is neglected. To take this into account Briaud and Smith (1984) has proposed a model where the ultimate soil resistance,  $p_u$ , is calculated as the sum of the net ultimate frontal resistance,  $Q$ , and the net ultimate side friction,  $F$ :

$$p_u = Q + F = (\eta P_{max} + \xi \tau_{max}) D \quad (37)$$

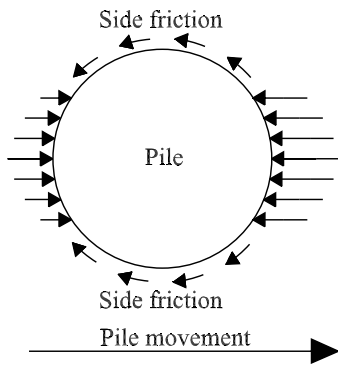


**Figure 21:** Side friction and soil pressure on the front and the back of the pile due to lateral deflection.

where  $P_{max}$  denotes the maximum frontal soil pressure acting on the pile,  $\tau_{max}$  denotes the maximum shear stress acting on the pile, and  $\eta$  and  $\xi$  are dimensionless constants. For circular piles Zhang et al.

(2005) recommends the use of (38)-(41) for  $P_{max}$ ,  $\tau_{max}$ ,  $\eta$  and  $\xi$ .

$$P_{max} = K_p^2 \gamma x \quad (38)$$

$$\tau_{max} = K \gamma x \tan(\delta) \quad (39)$$

$$\eta = 0.8 \quad (40)$$

$$\xi = 1.0 \quad (41)$$

Zhang et al. (2005) propose the side friction and frontal resistance to vary with depth similar to the variation proposed by Prasad and Chari (1999). They compared their method with small- and large-scale tests and found their method to be slightly conservative as the pile capacities calculated by their proposed method in average was 8 % smaller than the measured pile capacities. Further, parameters such as the embedded pile length, the slenderness ratio, the eccentricity ratio,  $e/L$ , and the friction angle did not affect the accuracy of their method, cf. fig. 22.

The importance of including side friction in the formulation of  $p-y$  curves is for the model proposed by Zhang et al. (2005) unaffected by the diameter since both the ultimate frontal resistance and the net ultimate side friction vary linearly with diameter. However, the ultimate frontal resistance varies non-linearly with diameter in the model proposed by Reese et al. (1974). The importance of side friction might therefore be more significant for large-diameter monopiles than for small-diameter piles.

## Summary

Several assumptions are employed when calculating the ultimate soil resistance according to Reese et al. (1974) and the design regulations, e.g. API (2000) and DNV (2010). These methods do not account for friction between pile and soil as the pile surface is assumed smooth. Furthermore, the failure modes are determined

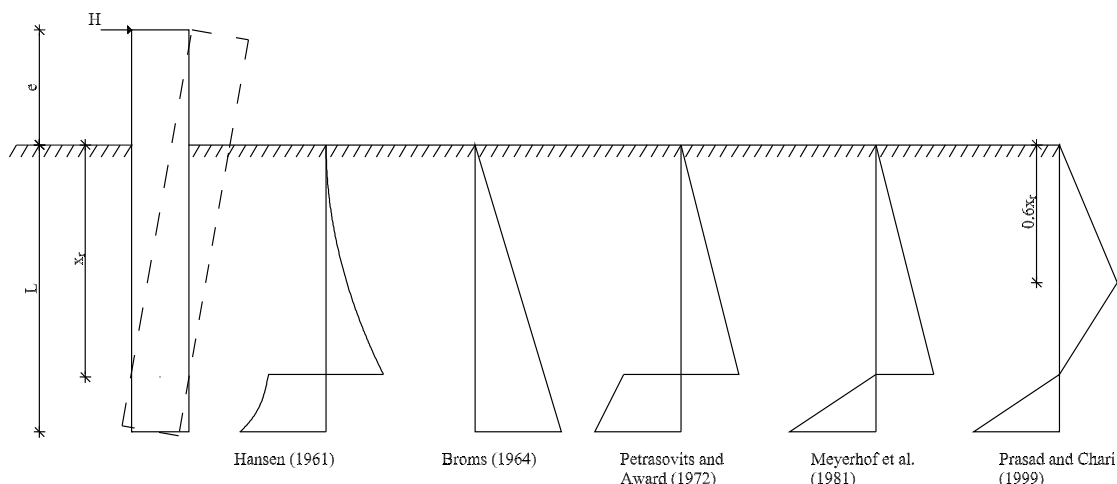


**Figure 20:** Sketch of the expressions of ultimate resistance proposed by Hansen et al. (1961), Broms (1964), Petrasovits and Award (1972), Meyerhof et al. (1981) and Prasad and Chari (1999), Zhang et al. (2005).

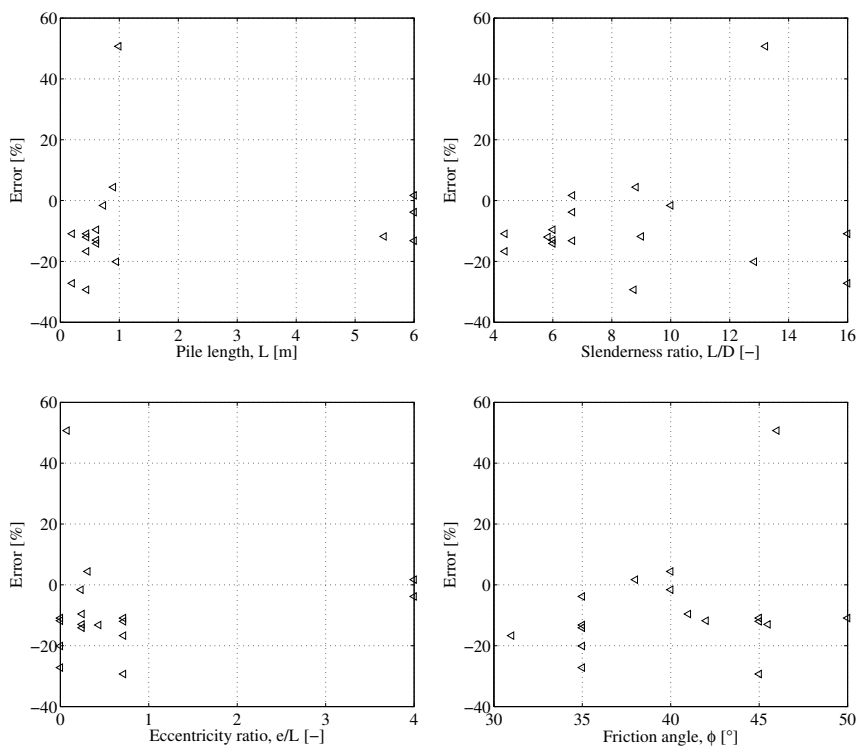


**Figure 22:** Error in percent between the predicted pile capacity estimated by means of the method by Zhang et al. (2005) and experimental tests, after Zhang et al. (2005)

for lateral pile translation. Hence, deflections beneath the point of zero pile deflection are accounted for in a very simplified manner. Thus, the assumed failure modes are inaccurate especially for non-slender piles.

The dilatancy of the soil affects the soil strength, but it is neglected in the expressions for the ultimate soil resistance.

Several methods for determining the ultimate soil resistance exist. The method proposed by Hansen (1961) were found to

correlate better with a finite element model than the methods proposed by Reese et al. (1974) and Broms (1964). In order to take the effect of side friction into account a model was proposed by Zhang et al. (2005) based on the findings of Briaud and Smith (1984) and Prasad and Chari (1999). Predictions regarding the ultimate soil resistance correlate well with laboratory and full-scale tests when using this model.

### 4.3 The influence of vertical load on lateral soil response

In current practice, piles are analysed separately for vertical and horizontal behaviour. Karthigeyan et al. (2006), Abdel-Rahman and Achmus (2006), Achmus et al. (2009a), and Achmus and Thieken (2010) investigated the effect of combined static vertical and lateral loading on the lateral and vertical pile response in sand through three-dimensional numerical modelling. Karthigeyan et al. (2006) adopted a Drucker-Prager constitutive model with a non-associated flow rule in their numerical modelling. Abdel-Rahman and Achmus (2006), Achmus et al. (2009a) and Achmus and Thieken (2010) all adopted the Mohr-Coulomb constitutive model with a non-associated flow rule. Further, they modelled the soil stiffness as stress-dependent.

Karthigeyan et al. (2006) calibrated the numerical model against two different kinds of field data carried out by Karasev et al. (1977) and Comodromos (2003). A concrete pile with a diameter of 0.6 m and a slenderness ratio of 5 were tested, cf. Karasev et al. (1977). The soil strata consisted of stiff sandy loam in the top 6 m underlain by sandy clay. Comodromos (2003) performed the tests in Greece. The soil profile consisted of silty clay near the surface with thin sublayers of loose sand. Beneath a medium stiff clay layer a very dense sandy gravel layer was en-

countered. A pile with a diameter of 1 m and a slenderness ratio of 52 were tested. A reasonable agreement between the field tests and the numerical model was found. Achmus and Thieken (2010) validated their numerical model against the model tests of Das et al. (1976) and Meyerhof and Sastry (1985). A good agreement were found. Abdel-Rahman and Achmus (2006) did not report whether their numerical model was validated against experimental tests. However, Abdel-Rahman and Achmus (2006) and Achmus and Thieken (2010) both used the commercial three-dimensional finite element programme ABAQUS and further they employed similar constitutive models. Therefore, the numerical model employed by Abdel-Rahman and Achmus (2006) is assumed also to fit the static model tests well.

To investigate the influence of vertical load on the lateral response in sand, Karthigeyan et al. (2006) modelled a squared concrete pile ( $1200 \times 1200$  mm) with a length of 10 m. Two types of sand were tested, a loose and a dense sand with friction angles of  $30^\circ$  and  $36^\circ$ , respectively. The vertical load was applied in two different ways, simultaneously with the lateral load (SAVL) and prior to the lateral load (VPL). Compressional vertical loading with values of 0.2, 0.4, 0.6, and 0.8 times the vertical pile capacity were applied. The conclusion of the analyses was that the lateral capacity of piles in sand increases under vertical loading. The increase in lateral capacity depended on how the vertical load was applied and on the relative density of the soil. The highest increase was in the case of VPL with a dense sand. For the dense sand with a lateral deflection of 5 % of the side length the increase in lateral capacity was, in the case of SAVL, of up to 6.8 %. The same situation in the case of VPL resulted in an increase of up to 39.3 %. Due to vertical loads higher vertical soil stresses and thereby higher horizontal stresses occur,

which also mobilise larger friction forces along the length of the pile. Therefore, the lateral capacity increases under the influence of vertical loading.

Abdel-Rahman and Achmus (2006), Achmus et al. (2009a) and Achmus and Thieken (2010) analysed the effect of combined vertical and lateral loading on both the vertical and lateral pile stiffness and capacity. Furthermore, they both considered compressive as well as tensile vertical loading. Abdel-Rahman and Achmus (2006) modelled the behaviour of hollow steel piles with pile diameters of 2.0 and 3.0 m and embedded pile lengths of 20 m, Achmus et al. (2009a) modelled concrete piles with diameters of 2.0 m and pile lengths of 10 and 30 m, while Achmus and Thieken (2010) modelled the behaviour of reinforced concrete piles with diameters of 0.5-3.0 m and embedded pile lengths of 15 m. They all considered piles installed in medium dense sand with a friction angle of  $35^\circ$ . The vertical and lateral loading was applied simultaneously. Abdel-Rahman and Achmus (2006) found that for axial compression the effect of combined loading increases both the pile lateral stiffness and pile lateral capacity, although the increase was very moderate. The vertical stiffness and capacity were found to increase significantly. The effect of combined loading was found to be more significant for rigid than flexible piles. This confirms the results reported by Karthigeyan et al. (2006). For axial tension no change were found in the lateral pile stiffness. However, the lateral pile capacity was found to decrease for combined loading. The vertical pile stiffness was found to decrease, while the vertical capacity was found to increase for combined lateral and vertical loading. The numerical modelling of Achmus et al. (2009a), and Achmus and Thieken (2010) confirmed the observations of Abdel-Rahman and Achmus (2006). Furthermore they presented interaction diagrams to be used for combined loading.

The above mentioned analysis of the effect of combined lateral and vertical loading on the lateral pile behaviour emphasize that both the vertical stiffness and capacity as well as the lateral stiffness and capacity are positively affected when the vertical loading is compressive. However, the effect is small when the vertical and lateral loads are applied simultaneously. Foundations for offshore wind turbines are exhibited to a constant vertical compressive load originating from the selfweight of the turbine and the foundation itself. In contrast, the horizontal loading is cyclic. Hence, the vertical loading is applied prior to the lateral loading, and combined loading might therefore significantly increase the pile stiffness and capacity of monopiles for offshore wind turbines. However, it should be emphasized that combined loading needs to be examined for cyclic loading and that the above mentioned findings needs to be examined further through experimental testing.

#### 4.4 Effect of soil-pile interaction

No importance is attached to the pile bending stiffness,  $E_p I_p$ , in the formulation of the  $p$ - $y$  curves. Hereby,  $E_{py}$  is independent of the pile properties, which seems questionable as  $E_{py}$  is a soil-pile interaction parameter. Another approach to predict the response of a flexible pile under lateral loading is the strain wedge (SW) model developed by Norris (1986). The method incorporates the pile properties. The concept of the SW model is that the traditional parameters in the one-dimensional Winkler approach can be characterised in terms of three-dimensional soil-pile interaction. The SW model was initially established to analyse free-headed piles embedded in uniform soils. Since then it has been improved such that it, for instance, can account for fixed pile head conditions, layered soils, soil liquefaction, pile group ef-

fects, and cyclic loading (Ashour et al., 1998; Ashour and Norris, 2000; Ashour et al., 2002; Ashour and Norris, 2003; and Lesny and Hinz, 2009).

The SW model parameters are related to a three-dimensional passive wedge developing in front of the pile subjected to lateral loading. The wedge has a form similar to the wedge associated with method A, as shown in fig. 9. However the angles  $\alpha$  and  $\beta$  are given by:

$$\alpha = \varphi_m \quad (42)$$

$$\beta = 45^\circ + \frac{\varphi_m}{2} \quad (43)$$

where  $\varphi_m$  is the angle of mobilised internal friction.

The purpose of the method is to relate the stresses and strains of the soil in the wedge to the subgrade reaction modulus,  $E_{py}$ . The SW model described by Ashour et al. (1998) assumes a linear deflection pattern of the pile over the passive wedge depth,  $h$ , as shown in fig. 23. The dimension of the passive wedge depends on two types of stability: local and global stability. To obtain local stability the SW model should satisfy equilibrium and compatibility between the pile deflection, the strains in the soil and the soil resistance acting on the pile wall. This is obtained by an iterative procedure where an initial horizontal strain in the wedge is assumed.

After assuming a passive wedge depth the subgrade reaction modulus can be calculated along the pile. Based on the calculated subgrade reaction modulus the pile-head deflection can be calculated from the one-dimensional Winkler approach. Global stability is obtained when concordance between the pile-head deflection calculated by the Winkler approach and the SW-model is achieved. The passive wedge depth is varied until global stability is obtained.

The pile bending stiffness influence the pile deflection pattern calculated by the

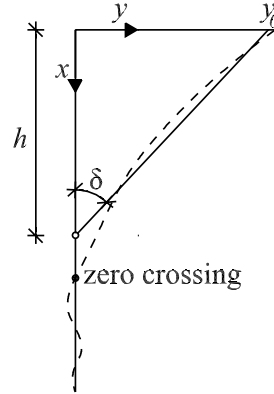


**Figure 23:** Linear deflection assumed in the SW-model, shown by the solid line. The dashed line shows the real deflection of a flexible pile. After Ashour et al. (1998).

one-dimensional Winkler approach and hereby also the wedge depth. Hence, the pile bending stiffness influences the  $p$ - $y$  curves calculated by the SW-model.

The equations associated with the SW model are based on the results of isotropic drained triaxial tests. Hereby an isotropic soil behaviour is assumed at the site. The SW model takes the real stresses into account by dealing with a stress level, defined as:

$$SL = \frac{\Delta\sigma_h}{\Delta\sigma_{hf}} \quad (44)$$

where  $\Delta\sigma_h$  and  $\Delta\sigma_{hf}$  are the mobilised horizontal stress change and the horizontal stress change at failure, respectively. The spread of the wedge is defined by the mobilised friction angle, cf. (42) and (43). Hence the dimensions of the wedge depends on the mobilised friction.

Although the SW model is based on the three-dimensional soil-pile interaction, and although it is dependent on both soil and pile properties, there are still significant uncertainties related to the model. The model does not take the active soil pressure that occurs at the back of the pile into account, which is a non-conservative consideration. Furthermore, the wedge only accounts for the passive soil pressure at the top front of the pile and neglects the passive soil pressure beneath the zero

crossing point which will occur for a non-slender pile, cf. section 4.2. The assumption of an isotropic behaviour of the soil in the wedge seems unrealistic in most cases for sand. To obtain isotropic behaviour the coefficient of horizontal earth pressure,  $K$ , needs to be 1, which is not the case for most sands.

Ashour et al. (2002) criticise the  $p$ - $y$  curve method as it is based and verified through a small number of tests. However, the SW model, has according to Lesny et al. (2007) been verified only for slender piles.

Ashour and Norris (2000) investigated by means of the SW model, the influence of pile stiffness on the lateral response for conditions similar to the Mustang Island tests.  $p$ - $y$  curves at a depth of 1.83 m are shown in fig. 24 for different values of  $E_p I_p$ . The  $p$ - $y$  curve proposed by Reese et al. (1974) is also presented in the figure. It is seen that there is a good concordance between the  $p$ - $y$  curve formulation proposed by Reese et al. (1974) and the SW model for similar pile properties. It should be noted that in fig. 24, the  $p$ - $y$  curve determined by means of the SW model depends on the pile bending stiffness such that an increase in the pile bending stiffness results in an increase in both the stiffness and the ultimate capacity of the  $p$ - $y$  curves. For other pile and soil properties, Ashour and Norris (2000), found that an increase in the pile bending stiffness led to less stiff  $p$ - $y$  curves. Hence, they conclude that the pile bending stiffness affects the  $p$ - $y$  curves, but that the effect is dependent on the type of soil and the type of loading. Furthermore, they found that the effect of pile bending stiffness on the SW  $p$ - $y$  curves is more significant for dense soils than for loose soils.

By means of the SW model Ashour and Norris (2000) found that the pile bending stiffness affects the shape of the  $p$ - $y$  curves significantly. Fan and Long (2005) investigated the effect of pile bending stiffness

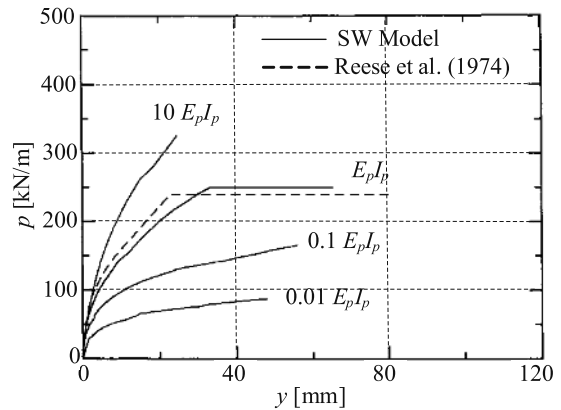


**Figure 24:** The influence of pile bending stiffness, after Ashour et al. (2000).

on the soil-pile interaction for piles situated in sand by means of numerical modelling. Fan and Long (2005) employed the constitutive model proposed by Desai et al. (1991). Both numerical models were validated against field tests. They calculated  $p$ - $y$  curves by integration of the normal and shear stresses in soil surrounding the pile. Fan and Long (2005) did not find an effect of the pile bending stiffness on the shape of the  $p$ - $y$  curves. In fig. 25  $p$ - $y$  curves calculated by means of the numerical model by Fan and Long can be observed for varying depth below soil surface and varying pile bending stiffness. For piles situated in clayey soil, Kim and Jeong (2011) found similar results. They also investigated the effect of pile bending stiffness by means of numerical modelling.

The conclusions of Fan and Long (2005) as well as Kim and Jeong (2011) contradicts the findings of Ashour and Norris (2000). More insight into the effect of the pile bending stiffness on the soil-pile interaction is therefore needed.

#### 4.5 Effect of diameter on initial stiffness of $p$ - $y$ curves

The initial modulus of subgrade reaction,  $k$ , is according to API (2000), DNV (2010), and Reese et al. (1974) only dependent on the relative density of the

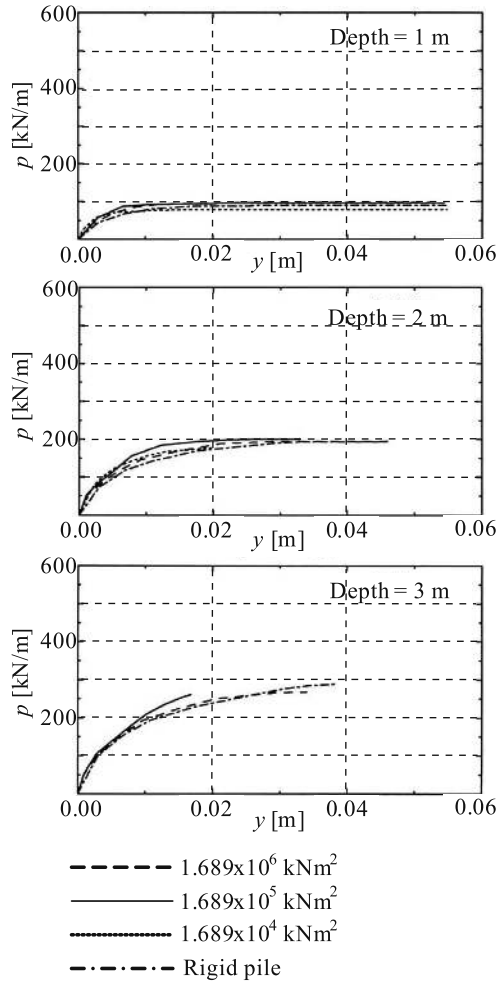


**Figure 25:** Effect of pile bending stiffness, after Fan and Long (2005).

soil. The dependency is shown in fig. 13. Hence, the methods A and B do not include  $E_p I_p$  and  $D$  in the determination of  $k$ . Different studies on the consequences of neglecting the pile parameters have been conducted over time with contradictory conclusions. Ashford and Juirnarongrit (2003) point out the following three conclusions in a summarization of previous research:

- Terzaghi (1955) analysed the effect of pile diameter on the modulus of subgrade reaction by consideration of stress bulbs forming in front of laterally loaded piles. Terzaghi concluded that by increasing the pile diameter the stress bulb formed in front of the

pile is stretched deeper into the soil. This results in a greater deformation due to the same soil pressure at the pile. Terzaghi therefore postulated that the soil pressure acting on the pile wall is linearly proportional to the inverse of the pile diameter giving that the modulus of subgrade reaction,  $E_{py}$ , is independent on the diameter.

- Vesic (1961) proposed a relation between the modulus of subgrade reaction used in the Winkler approach and the soil and pile properties. This relation showed that  $E_{py}$  is independent of the diameter for circular and squared piles.
- Pender (1993) refers to two reports conducted by Carter (1984) and Ling (1988). Assuming a simple hyperbolic soil model for the relationship between soil resistance and pile deflection, they backcalculated values of  $E_{py}^*$  and  $p_u$  from field tests. In the backcalculation they assumed that Young's modulus of elasticity of the soil and therefore also the initial subgrade reaction modulus were constant with depth. Based on the backcalculations they proposed an expression of  $E_{py}^*$  which is linearly proportional to the pile diameter.

Pender et al. (2007) comments on the research of Carter (1984) and Ling (1988) and their conclusion of  $E_{py}^*$  varying linearly with pile diameter. Pender et al. (2007) questions the validity of a constant value of  $E_s$  with depth. Instead they propose  $E_s$  to be proportional to either the square root of the depth or to the depth. They suggests that the findings of Pender (1993) was due to a false assumption of the variation of Young's modulus of elasticity with depth. They, conclude that  $E_{py}^*$  is independent of the pile diameter.

The conclusions made by Terzaghi (1955) and Vesic (1961) concerns the subgrade re-

action modulus,  $E_{py}$ , while the conclusions made by Pender (1993) concerns the initial modulus of subgrade reaction,  $E_{py}^*$ . The conclusions of Terzaghi (1955) and Vesic (1961) might also be applicable for the initial modulus of subgrade reaction,  $k$ , and the initial stiffness,  $E_{py}^*$ .

Based on the investigations presented by Terzaghi (1955), Vesic (1961), Pender (1993), and Pender et al. (2007), it must be concluded that no clear correlation between the initial modulus of subgrade reaction and the pile diameter has been realised. Ashford and Juirnarongrit (2005) contributed to the discussion with their extensive study of the problem which was divided into three steps:

- Numerical modelling by means of a simple finite element model.
- Analyses of vibration tests on large-scale concrete piles.
- Back-calculation of  $p$ - $y$  curves from static load tests on the concrete piles.

The finite element analysis was according to Ashford and Juirnarongrit (2005) very simple and did not account very well for the soil-pile interaction since friction along the pile, the effect of soil confinement, and gaps on the back of the pile were not included in the model. In order to isolate the effect of the diameter on the magnitude of  $E_{py}$ , the bending stiffness of the pile was kept constant when varying the diameter. The conclusion of the finite element analysis were that the diameter had some effect on the pile-head deflection as well as the moment distribution. An increase in diameter led to a decreasing pile-head deflection and a decreasing depth to the point of maximum moment. However, Ashford and Juirnarongrit (2005) concluded that the effect of increasing the diameter appeared to be relatively small compared to the effect of increasing the bending stiffness,  $E_p I_p$ .

The second part of the work by Ashford and Juirnarongrit (2005) dealt with vibration tests on large-scale monopiles. The tests included three instrumented piles with diameters of 0.6, 0.9, and 1.2 m (12 m in length) and one pile with a diameter of 0.4 m and a length of 4.5 m. All piles were cast-in-drilled-hole and made up of reinforced concrete. They were installed at the same site consisting of slightly homogenous medium to very dense weakly cemented clayey to silty sand. The piles were instrumented with several types of gauges, i.e. accelerometers, strain gauges, tiltmeters, load cells, and linear potentiometers. The concept of the tests were that by subjecting the piles to small lateral vibrations, the soil-pile interaction at small strains could be investigated.

Based on measured accelerations, the natural frequencies of the soil-pile system were determined. These frequencies were in the following compared to the natural frequencies of the system determined by means of a numerical model. Two different expressions for the modulus of subgrade reaction,  $E_{py}$ , were used: one that is linearly dependent; and one that is independent on the diameter. The strongest correlation was obtained between the measured frequencies and the frequencies computed by using the relation independent of the diameter. Hence, the vibration tests substantiate Terzaghi and Vesic's conclusions. It is noticed that the piles were only subjected to small deflections, hence  $E_{py} \approx E_{py}^*$ .

Finally, Ashford and Juirnarongrit (2005) performed a back-calculation of  $p$ - $y$  curves from static load cases. From the back-calculation a soil resistance was found at the ground surface. This is in contrast to the  $p$ - $y$  curves for sand given by Reese et al. (1974) and the recommendations in API (2000) and DNV (2010) in which the initial stiffness,  $E_{py}^*$ , at the ground surface is zero. The resistance at the ground surface might be a consequence of cohesion in



the slightly cemented sand or a result of magnification of measurement uncertainties when double-differentiating the strain-gauge measurements.

Furthermore, a comparison of the results from the back-calculations for the various pile diameters indicated that the effects of pile diameter on  $E_{py}^*$  were insignificant. The three types of analyses conducted by Ashford and Juirnarongrit (2005) therefore indicate the same: the effect of the diameter on  $E_{py}^*$  is insignificant.

Fan and Long (2005) investigated the influence of the pile diameter on the soil response by means of numerical modelling. They employed the constitutive model proposed by Desai et al. (1991) and a non-associative flow rule in their numerical model. By varying the diameter and keeping the bending stiffness,  $E_p I_p$ , constant in their finite element model they investigated the influence of the pile diameter on the initial subgrade reaction modulus. The results are given as curves normalised by the diameter and vertical effective stress as shown in fig. 26. No significant correlation between diameter and initial stiffness is observed. It must be emphasised that the investigation considered only slender piles.

For non-slender piles the bending stiffness might cause the pile to deflect almost as a rigid object. Therefore, the deflection at the pile-toe might cause a significant soil resistance near the pile toe. Thus a correct prediction of the variation of initial stiffness with depth is important in order to determine the correct pile deflection.

Based upon a design criterion demanding the pile to be fixed at the toe, Lesny and Wiemann (2006) investigated by back-calculation the validity of the assumption of a linearly increasing  $E_{py}^*$  with depth. The investigation indicated that  $E_{py}^*$  is overestimated for large-diameter piles at great depths. Therefore, they suggested a power function, to be used instead of a

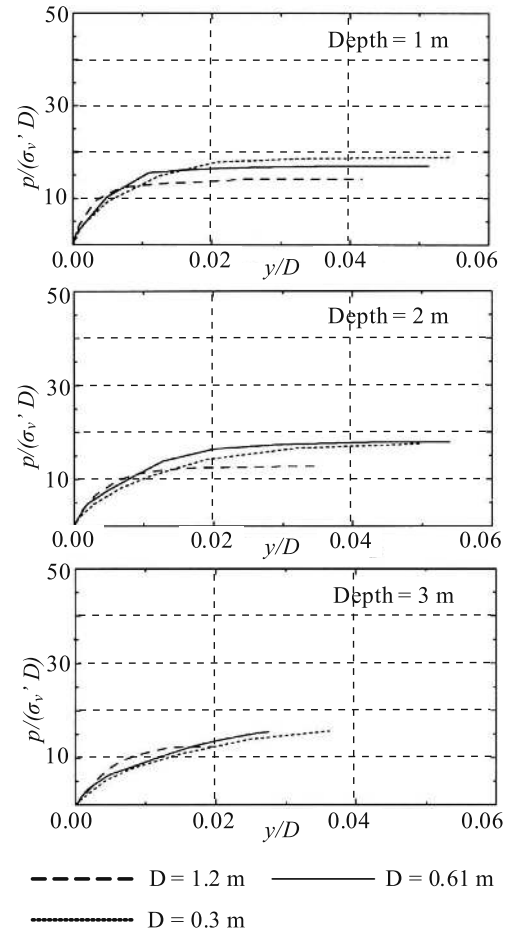


**Figure 26:** Effect of changing the diameter, after Fan and Long (2005).

linear relation, cf. fig. 27. A finite element model was made in order to validate the power function. The investigations showed that employing the power function approach gave deflections more similar to the numerical modelling than by using the traditional linear approach in the  $p$ - $y$  curve method. However, it was emphasised that the method should only be used for determination of pile length. The  $p$ - $y$  curves still underestimates the pile-head deflections even though the parabolic approach is used.

The above mentioned investigations all made by means of cohesionless soils are summarised in tab. 4. From this tabular it is obvious that more research is needed.

Looking at cohesive materials the tests are also few. According to Ashford

**Table 4:** Chronological list of investigations concerning the effects of diameter on the initial stiffness of the  $p$ - $y$  curve formulations.

Author	Method	Conclusion
Terzaghi (1955)	Analytical	Independent
Vesic (1961)	Analytical	Independent
Carter (1984)	Analytical expression calibrated against full-scale tests	Linearly dependent
Ling (1988)	Validation of the method proposed by Carter (1984)	Linearly dependent
Ashford and Juirnarongrit (2005)	Numerical and large-scale tests	Insignificant influence
Fan and Long (2005)	Numerical	Insignificant influence
Lesny and Wiemann (2006)	Numerical	Initial stiffness is non-linear for long and large-diameter piles
Pender et al. (2007)	Analytical expression calibrated against full-scale tests	Independent

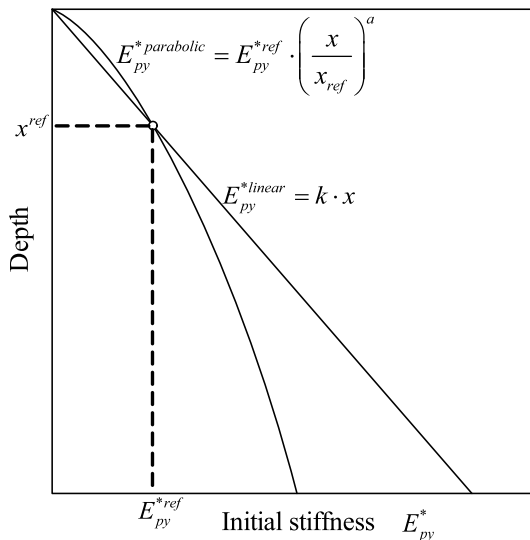


**Figure 27:** Variation of initial stiffness,  $E_{py}^*$ , as function of depth, after Lesny and Wiemann (2006). The linear approach is employed in Reese et al. (1974) and the design codes, e.g. API (2000) and DNV (2010). The exponent  $a$  can be set to 0.5 and 0.6 for dense and medium dense sands, respectively.

and Juirnarongrit (2005) the most significant findings are presented by Reese et al. (1975), Stevens and Audibert (1979), O'Neill and Dunnavant (1984), and Dunnavant and O'Neill (1985).

Reese et al. (1975) back-calculated  $p$ - $y$  curves for a 0.65 m diameter pile in order to predict the response of a 0.15 m pile. The calculations showed a good approximation of the moment distribution, but the deflections however were considerably underestimated compared to the measured values associated with the 0.15 m test pile.

Based on published lateral pile load tests Stevens and Audibert (1979) found that deflections computed by the method proposed by Matlock (1970) and API (1987) were overestimated. The overestimation increases with increasing diameter leading to the conclusion that the modulus of subgrade reaction,  $E_{py}$ , increases for increasing diameter.

By testing laterally loaded piles with diameters of 0.27 m, 1.22 m, and 1.83 m in an overconsolidated clay, O'Neill and Dunnavant (1984) and Dunnavant and O'Neill (1985) found that there were a non-linear relation between deflection and diameter. They found that the deflection at 50 %

of the ultimate soil resistance generally decreased with an increase in diameter. Hence,  $E_{py}$  increases with increasing pile diameter.

Kim and Jeong (2011) and Jeong et al. (2011) investigated the effect of pile diameter on the initial stiffness through numerical modelling. They considered piles situated in clay. They found that the initial stiffness of the  $p$ - $y$  curves increases linearly with the square root of the pile diameter.

#### 4.6 Choice of horizontal earth pressure coefficient

When calculating the ultimate soil resistance by method A the coefficient of horizontal earth pressure at rest,  $K_0$ , equals 0.4 even though it is well-known that the relative density/the internal friction angle influences the value of  $K_0$ . In addition, pile driving may increase the coefficient of horizontal earth pressure  $K$ .

The influence of the coefficient of horizontal earth pressure,  $K$ , is evaluated by Fan and Long (2005) for three values of  $K$  and an increase in ultimate soil resistance were found for increasing values of  $K$ . The increase in ultimate soil resistance is due to the fact, that the ultimate soil resistance is primarily provided by shear resistance in the sand, which depends on the horizontal stress.

Reese et al. (1974), and O'Neill and Murchison (1983) and thereby also API (2000) and DNV (2010) consider the initial modulus of subgrade reaction  $k$  to be independent of  $K$ . Fan and Long (2005) investigated this assumption. An increase in  $K$  results in an increase in confining pressure implying a higher stiffness. Hence,  $k$  is highly affected by a change in  $K$  such that  $k$  increases with increasing values of  $K$ .

#### 4.7 Shearing force at the pile-toe

Recently installed monopiles have diameters around 4 to 6 m and a pile slenderness ratio around 5. Therefore, the bending stiffness,  $E_p I_p$ , is quite large compared to the pile length. The pile curvature will therefore be small and the pile will almost behave as a rigid object as shown in fig. 28.

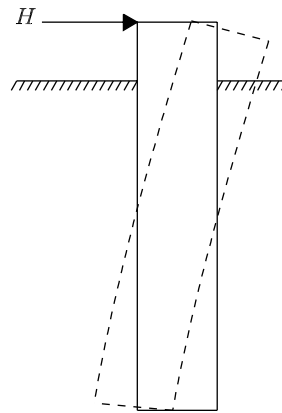


Figure 28: Deflection curve for non-slender pile.

As shown in fig. 28 there is a significant negative deflection at the pile-toe. This deflection causes shearing stresses at the pile-toe to occur, which increase the total lateral resistance. According to Reese and Van Impe (2001) a number of tests have been made in order to determine the shearing force at the pile-toe, but currently no results from these tests have been published and no methods for calculating the shearing force as a function of the pile toe deflection have been proposed.

Due to rigid pile behaviour normal stresses at the pile toe will inflict a bending moment on the pile toe resulting in a bigger pile stiffness and capacity. Research is needed to establish a relationship between the pile toe rotation and the applied moment at the pile toe.

## 4.8 Shape of $p$ - $y$ curves

Currently, a tangent hyperbolic function is employed to describe the shape of  $p$ - $y$  curves for piles in sand, cf. (29) and O'Neill and Murchison (1983). Other shapes of  $p$ - $y$  curves has also been proposed to describe the relationship between the soil resistance acting on the pile wall and the pile deflection, for instance, Reese et al. (1974), Scott (1980), PHRI (1980), and Carter (1984). Reese et al. (1974) suggested the use of a piecewise curve consisting of an initial straight line, a parabola, and a straight line. These three curves were assembled into one continuous piecewise differentiable curve, cf. Method A. Scott (1980) proposed a  $p$ - $y$  curve for sand consisting of two straight lines. His recommendation was based on centrifuge tests of laterally loaded piles. The expression of Scott (1980) is not bounded by an upper limit. Hence, the ultimate soil resistance is not considered in that method. Murchison and O'Neill (1984) compared these three expressions with a series of field tests on flexible piles and found the tangent hyperbolic function to fit best with the tests. Carter (1984) proposed the use of a hyperbolic expression for  $p$ - $y$  curves in sand:

$$p(y)^n = \frac{y}{1/E_{py}^* + y/p_u^n} \quad (45)$$

where  $n$  is a dimensionless constant. Carter (1984) proposed to use  $n = 1$  for sand and  $n = 0.2$  for clay. Ling (1988) confirmed the hyperbolic expression by comparison with 28 full-scale tests on flexible piles.

PHRI (1980) proposes the use of a  $p$ - $y$  curve formulation in which the soil resistance is proportional with the square of the pile deflection. Hence, this  $p$ - $y$  curve formulation is not bounded by an upper limit. Terashi (1989) found a good agreement between this  $p$ - $y$  curve expression

and centrifuge tests on flexible piles situated in dense sand.

The accuracy of the  $p$ - $y$  curves proposed by O'Neill and Murchison (1983), Carter (1984), and PHRI (1980) needs to be compared and validated for non-slender piles.

## 4.9 Layered soil

The  $p$ - $y$  curve formulations of Reese et al. (1974), Murchison and O'Neill (1974), etc. considers piles situated in homogeneous soil. However, the soil stratification is rarely homogeneous. A few analytical studies on the effect of layered soils have been conducted, for instance, Davisson and Gill (1963), Khadilkar et al. (1973), Naik and Peyrot (1976), and Dordi (1977). However, these analyses do not consider the non-linearity of the soil.

Georgiadis (1983) proposed a new approach to develop  $p$ - $y$  curves in a layered soil stratification. The approach involves the determination of an equivalent depth,  $h$ , for all soil layers existing below the upper soil layer. The equivalent depth of layer  $i$  is determined by solving  $h_i$  in the following equation:

$$F_1 + \dots + F_{i-1} = F_i \Rightarrow \quad (46)$$

$$\int_0^{H_1} p_u dx + \dots + \int_{h_{i-1}}^{h_{i-1}+H_{i-1}} p_u dx = \int_0^{h_i} p_u dx \quad (47)$$

where  $F_1$  is the sum of the ultimate soil resistance for layer 1,  $F_{i-1}$  is the sum of the ultimate soil resistance for the  $(i-1)$ 'th, and  $F_i$  is the sum of the ultimate soil resistance for the  $i$ 'th layer.  $H_1$ ,  $H_{i-1}$ , and  $H_i$  are the layer thickness of soil layer 1,  $i-1$ , and  $i$ , respectively.  $h_{i-1}$  and  $h_i$  are the equivalent depth of the soil layers  $i-1$  and  $i$ .

Georgiadis (1983) validated his method against a field test at Lake Austin on a pile with a diameter of 0.152 m and an embedded pile length of 4.9 m. Hence, the length to diameter ratio was 32.2 and the pile can be considered as flexible. The soil stratification at the site consisted of 0.38 m of stiff clay overlying a medium dense sand layer. The proposed method for layered soil fitted the field test very well.

It should be emphasized that the method of Georgiadis (1983) for deriving  $p$ - $y$  curves for layered soils is developed and validated for flexible piles. The method still needs validation for piles behaving rigidly.

Based on numerical analyses Yang and Jeremic (2005) as well as McGann et al. (2012) investigated laterally loaded piles situated in a layered soil stratification. Yang and Jeremic (2005) modelled the behaviour of a flexible square pile situated in a stratification of sand and soft clay. They conducted numerical simulations with both a sand-clay-sand and a clay-sand-clay stratification. The analysis of McGann et al. (2012) is based on circular piles situated in seismic areas exposed to lateral spreading. They considered piles installed in sands with a loose liquified intermediate layer.

Yang and Jeremic (2005) used von Mises constitutive model to model the clay and the Drucker-Prager constitutive model for the sand. They modelled a pile with a width of 0.429 m and a length of 13.7 m. Hence, the slenderness ratio was 31.9. Similar to Georgiadis (1983) they found that the upper layers affected the  $p$ - $y$  curves of the lower layers. Further, they found that the lower layers also affected the  $p$ - $y$  curves of the upper layers in such a way that the  $p$ - $y$  curves of a stiff upper layer are reduced near a soft intermediate layer. The size of the reduction was found to depend on the distance to the interlayer, such that the largest reduction took place

at the interlayer. For the clay-sand-clay stratification they found that the stiff intermediate layer resulted in increased soil resistance in the upper clay layer.

McGann et al. (2012) used the Drucker-Prager constitutive model in their numerical model. They modelled a circular pile with a diameter varying from 0.61 m to 2.5 m. Similar to Yang and Jeremic (2005) they found that the intermediate layer affects the soil resistance of the upper layer. According to McGann et al. (2012) the stiff soil near the interface of the weaker intermediate layer can be pushed into the weaker layer as the pile deflects laterally. This explains the reduction in the soil resistance of the stiff soil layers.

Based on their numerical simulations, McGann et al. (2012) presented an expression for the reduction of the soil resistance of the upper and lower layer. The reduction depends exponentially on the distance from the intermediate layer. Other parameters such as the pile diameter, the depth of the intermediate layer, the friction angle of the upper and lower layers, and the thickness of the intermediate layer were also included in the expression for the reduction. The analysis of McGann et al. (2012) considered the intermediate layer as liquefied. Their expression is therefore only validated for stratifications with an intermediate layer which is liquefied. The expression might however also be valid in stratifications where the intermediate layer is significantly softer than the upper and lower layers, for instance stratifications with an organic intermediate layer.

#### 4.10 Long-term cyclic loading

Offshore wind turbines are exposed to cyclic loading from the wind and wave forces. During the lifetime of an offshore wind turbine the foundation will be exposed to a few number of load cycles with

large amplitudes due to storms and further to  $10^6$ - $10^8$  load cycles with low or intermediate amplitudes. The ratio between the minimum and maximum load in each cycle,  $\zeta_c$ , will vary with time. The ratio between the maximum load in each cycle and the static pile capacity is in the following denoted as  $\zeta_b$ . When designing monopile foundations for offshore wind turbines it should be ensured that the accumulated pile rotation is less than the value specified by the wind turbine supplier. Similarly, it should also be ensured that the natural frequency of the combined structure is within the range specified by the wind turbine supplier. Typically, the foundation is designed such that the natural frequency of the combined structure is within the rotor frequency and the blade passing frequency. According to LeBlanc (2009), wind turbines are often designed such that the rotor frequency is in the range of 0.17-0.33 Hz, while the blade passing frequency typically is in the range of 0.5-1.0 Hz. The energy rich wind turbulence lies below a frequency of 0.1 Hz, and the frequency of extreme waves is typically in the range of 0.07-0.14 Hz. When a pile is exposed to cyclic loading, the stiffness of the soil might change due to a reconfiguration of the soil particles. Therefore, knowledge regarding the influence of cyclic loading on the stiffness of the soil-pile interaction is necessary for accurate determination of the accumulated pile rotation and of the variation of the natural frequency for the combined structure with time.

The  $p$ - $y$  curve formulations proposed by Reese et al. (1974) and O'Neill and Murchison (1983) accounts for cyclic loading by means of reductions of the empirical factors  $A$  and  $B$ . Hence, the accumulated pile deflection is accounted for, however, in a very simplified manner. Changes in the initial stiffness of the  $p$ - $y$  curves is not accounted for, since  $A$  only affect the upper limit of soil resistance (Method A and B), and  $B$  the soil resistance at a pile deflection of  $y = D/60$  (Method A). The param-

eters  $A$  and  $B$  for cyclic loading are based on few tests on flexible piles with up to approximately 100 load cycles. Further, the influence of relative density, installation method, number of cycles, etc. are not included in the expression of  $A$  and  $B$  for cyclic loading. Hence, these  $p$ - $y$  curve formulations are incomplete in describing the cyclic pile behaviour of monopile foundations for offshore wind turbines.

The behaviour of laterally loaded piles subjected to cyclic loading has been investigated by means of experimental testing and numerical modelling. The major findings are summarised in the following. The pile and soil properties as well as loading conditions for the experimental testing which is referred to regarding the behaviour of cyclically loaded piles are summarised in tab. 5.

Long and Vanneste (1994) summarises previous research regarding the behaviour of cyclically loaded piles:

- Prakash(1962), Davisson and Salley (1970), and Alizadeh and Davisson (1970) considered the cyclic pile response based on model and field tests. Prakash (1962) and Davisson and Salley (1970) conducted model tests on aluminium pipe piles with outer diameters of 12.7 mm (0.5 in) and embedded pile lengths of 0.533 m (21 in). Hence the slenderness ratio is 40 and the piles can be considered as flexible. The piles were situated in medium dense dry sand. Alizadeh and Davisson (1970) conducted field tests on a pile with an outer diameter of 0.4 m and a slenderness ratio of 40. The pile was situated in a layered soil consisting of silty sand to gravelly sand. Prakash (1962), Davisson and Salley (1970) as well as Alizadeh and Davisson (1970) concluded that for 50 or more load cycles the cyclic stiffness of the modulus of subgrade reaction is approximately 30 % of the

**Table 5:** Pile, soil and loading properties for the model and field tests used for investigation of the behaviour of cyclically loaded piles.

	Pile diameter $D$ [m]	Embedded pile length $L$ [m]	Slenderness ratio $L/D$ [-]	Soil compaction	$\zeta_b$ [-]	$\zeta_c$ [-]	$N$ [-]
Cox et al. (1974)/ Reese et al. (1974)	0.61	21.0	34	medium dense to very dense		(-1)- (-0.25)	0-100
Prakash (1962)	0.0127	0.533	40	Medium dense			100
Davisson and Salley (1970)	0.0127	0.533	40	Medium dense			4
Alizadeh and Davisson (1970)	0.400	16	40	Loose		0	100
Little and Briaud (1988b)	0.510- 1.065	29.6- 39.0	32-60	Medium dense		0- 0.5	21
Long and Vanneste (1994)	0.145- 1.430	3.8- 39.0	3-84	Loose to dense		(-1.0)- 0.5	5- 500
Lin and Liao (1999)	0.145- 1.430	5.0- 21.0	4-84	Loose to dense		(-1.0)- 0.1	4- 100
Peng et al. (2006)	0.0445	0.400	9	Medium dense	0.2- 0.6	(-1)- (-0.6)	10000
Peralta and Achmus (2010)	0.060- 0.063	0.200- 0.500	3-8	Medium dense		0	10000
LeBlanc et al. (2010a)	0.080	0.360	4.5	very loose to loose	0.20- 0.53	(-1.0)- 1.0	7000- 65000
LeBlanc et al. (2010b)	0.080	0.360	4.5	very loose to loose	0.28- 0.53	0	100- 10000

static stiffness.

- Broms (1964) similarly considered the cyclic pile behaviour based on the subgrade reaction method. He found that the degradation of the static stiffness depends on the relative density of the soil, such that the stiffness is reduced to 25 % of the static stiffness for loose soils and to 50 % for dense soils. The mentioned reductions in subgrade reaction modulus was for 40 load cycles.
- Little and Briaud (1988b) proposed to degrade the soil resistance in the  $p$ - $y$  curve formulation with the number of load cycles by means of an ex-

ponential expression:  $p_c = p_s N^{-a}$ . The cyclic soil resistance is denoted  $p_c$ , the static soil resistance is denoted  $p_s$ , the number of load cycles is denoted  $N$  and  $a$  is an empirical factor. The expression was validated against 12 pressuremeter tests on model piles with outer diameters of 34.5 mm (1.36 in) situated in dry sand. Further, the expression was validated against six field tests on pipe piles driven or drilled into the soil. The piles had outer diameters of 0.510 m to 1.065 m, embedded pile lengths of 29.6 to 39.0 m and slenderness ratios of 32 to 60. The piles therefore exhibited a slender pile behaviour. The pile slender-

ness ratio varied from 37 to 59. The piles were installed in medium dense sand.

Long and Vanneste (1994) analysed 34 field tests on piles exposed to cyclic lateral loading. The pile dimensions were  $D = 0.145 - 1.43$  m,  $L_p = 3.8 - 39.0$  m,  $L_p/D = 3 - 84$ . Various pile cross-sections and installation methods were used for the 34 field tests. The soil compaction varied from loose to dense and the number of load cycles varied from 5 to 500. Based on back-analyses of the field tests, they proposed to degrade the static  $p$ - $y$  curve formulation proposed by Reese et al. (1974) in the following way to account for cyclic loading:

$$p_N = p_1 * N^{-0.4t} \quad (48)$$

$$y_N = y_1 * N^{0.6t} \quad (49)$$

where  $p_N$  is the soil resistance after  $N$  cycles,  $p_1$  is the static soil resistance,  $y_N$  is the pile deflection after  $N$  cycles,  $y_1$  is the static pile deflection, and  $t$  is a dimensionless parameter. The dimensionless parameter  $t$  was found to depend primarily on  $\zeta_c$ , but also the installation method and the relative density were found to exhibit a minor influence on  $t$ . They found that  $t$  assumes the largest values for one-way cyclic loading with  $\zeta_c = 0.0 - 0.5$ .

Lin and Liao (1999) proposed a method for determination of the accumulated pile displacement caused by mixed lateral loading. Their method is based on the expression for the cumulative strains due to mixing of different amplitude loads proposed by Stewart (1986) and on Miner's rule (Miner, 1945). In their method, they assume that the representative lateral strain can be calculated from the pile deflection as  $\epsilon = y/(2.5D)$ . This relationship between the lateral strain and the pile deflection was originally suggested by Kagawa and Kraft (1980). Lin and Liao (1999) suggest that the relationship,  $R_s$ , between the lateral strain after  $N$  cycles,  $\epsilon_N$ , and

the lateral strain after one cycle,  $\epsilon_1$ , is given as:

$$R_s = \frac{\epsilon_N}{\epsilon_1} = 1 + t \ln(N) \quad (50)$$

where  $t$  depends on the relative density, the installation method,  $\zeta_c$  and the ratio between the pile length and the pile/soil relative stiffness,  $T$ . They calibrated the parameter  $t$  against 20 field tests on piles with outer pile diameters of 0.145-1.43 m, embedded pile lengths of 5.0-21.0 m and slenderness ratios of 4-84. The installation method varied and further the soil compaction varied from loose to dense. They validated their method against the field tests presented by Little and Briaud (1988b). A reasonable agreement were found with the tests. It should be noted that the number of load cycles in the field tests were limited to a maximum of 100 cycles.

Peng et al. (2006) invented a new testing device for cyclic loading of laterally loaded piles. By means of the new testing device they conducted two-way cyclic tests with 10000 cycles and both balanced and unbalanced cyclic loading. They concentrated on the development of the innovative testing device and only presented few results from cyclic load tests. The test results they presented were for a pile with an outer diameter of 44.5 mm, an embedded pile length of 400 mm and a slenderness ratio of 9. The pile was situated in a dry sand with  $I_D = 71.7$  %. The loading frequency were varied from 0.45-0.94 Hz. The applied cyclic loading had  $\zeta_b = 0.2 - 0.6$  and  $\zeta_c = (-1) - (-0.6)$ . They concluded that the pile displacement increases for increasing loading frequency. Whether this was due to resonance between the natural frequency of the pile and the loading was not discussed. They found that the accumulated pile displacement is significantly greater for unbalanced loading than balanced loading, which is similar to the findings of Long and Vanneste (1994) and Lin and Liao (1999). Further,



they found that within 10000 load cycles the accumulated pile deflection continued to increase.

Lesny and Hinz (2007) proposed to model the cyclic pile behaviour by means of a combination of finite element modelling and cyclic triaxial testing. They implemented the results from undrained, unconsolidated, stress-controlled cyclic triaxial tests in the constitutive model. The method for the finite element modelling of the cyclic pile behaviour includes the following steps:

- At first the variation of load versus number of load cycles is estimated. The loading is divided into a number of load levels each with a corresponding number of load cycles.
- For varying load levels the induced states of stresses in the soil is calculated by finite element analysis using soil parameters for static loading.
- Triaxial tests are conducted according to the determined stress conditions.
- The accumulated plastic strain per load level is calculated, and their sum is determined with use of Miner's rule (Miner, 1945).
- The soil properties are modified to account for the cyclic behaviour, and the pile behaviour is determined by means of finite element modelling employing the updated soil parameters.

The method proposed by Lesny and Hinz (2007) needs to be validated against cyclic tests on laterally loaded piles.

Achmus et al. (2009b) analysed the cyclic pile behaviour of non-slender large-diameter piles through numerical modelling employing the Mohr-Coulomb constitutive model. The cyclic behaviour of the soil was implemented through a degrading soil stiffness. The formulation

proposed by Huurman (1996), which is based on triaxial testing of cohesionless soil, was applied to express the stiffness degradation. Achmus et al. (2009b) presented a parametrical study on the accumulation of pile deflection due to cyclic loading in which the pile diameter, the pile length, the loading eccentricity, the relative density and  $\zeta_b$  was varied within  $D = 2.5 - 7.5$  m,  $L = 20 - 40$  m,  $e = 0 - 40$  m, medium dense to dense sand and  $\zeta_b = 0 - 0.6$ . For all the simulations one-way loading with  $\zeta_c = 0$  were applied. Based on the parametric study they presented design charts relating the ratio between the static and cyclic pile deflection (accumulation rate of deformation) with  $\zeta_b$  for varying numbers of load cycles. They found that the pile diameter, the embedded pile length, and the relative soil density affect the accumulation rate of deformation through their effect on the static pile capacity and hence also their effect on the normalized load.

Peralta and Achmus (2010) conducted a series of 1-g tests on both flexible and rigid piles in order to investigate the behaviour of cyclic loaded piles. The pile dimensions was  $D = 60 - 63$ mm and  $L = 200 - 500$ mm. The pile material employed for the tests varied from steel to high density poly-ethylene (HDPE). The piles made of HDPE behaved as slender piles due to the significantly lower Young's modulus of elasticity for HDPE. One-way cyclic loading with  $\zeta_c = 0$  were considered. For each test, the 10000 load cycles were applied. They attempted to fit both an exponential and a logarithmic expression for the accumulation of displacement to the test results, as proposed by Long and Vanneste (1994) and Lin and Liao (1999), respectively. They concluded that the exponential function for the displacement accumulation fitted well with the experimental tests on rigid piles while the logarithmic expression fitted the flexible piles well. They presented a comparison of the evaluation of accumulated pile deflec-

tion for two equivalent irregular load patterns: one in which the cyclic load amplitude ascended; and one in which the cyclic load amplitude descended. From the comparison it could be observed that the accumulated load displacement was approximately 25 % higher for the irregular cyclic load pattern with ascending loads than the pattern with descending loads.

LeBlanc et al. (2010a) and LeBlanc et al. (2010b) investigated the cyclic behaviour of non-slender piles through small-scale testing at 1-g. They tested a pile with an outer diameter of 80 mm and an embedded pile length of 360 mm. The slenderness ratio was hereby 4.5 implying rigid pile behaviour. They conducted tests at relative soil densities of 4 and 38 %. The pile was exposed to a series of cyclic load tests with varying  $\zeta_b$  and  $\zeta_c$ .  $\zeta_b$  was varied between 0.2 and 0.53, while  $\zeta_c$  was varied from -1 to 1. The values of  $\zeta_b$  corresponds to loads ranging from the fatigue limit state (FLS) to the serviceability limit state (SLS).

LeBlanc et al. (2010a) considered the accumulated pile rotation and the change in pile stiffness for continuous long-term cyclic loading. Regarding the accumulated pile rotation, they proposed the following expression:

$$\frac{\Delta\theta(N)}{\theta_s} = T_b(\zeta_b, I_D) T_c(\zeta_c) N^{0.31} \quad (51)$$

where  $T_b$  and  $T_c$  are dimensionless functions. They found that  $T_b$  increases for increasing values of both  $\zeta_b$  and  $I_D$ , while they proposed a nonlinear variation of  $T_c$  with  $\zeta_c$ . For  $\zeta_c$  equal to either -1 or 1, e.i. two-way cyclic loading with a mean value of 0 and static loading, respectively, they suggested that  $T_c$  is 0, while for  $\zeta_c = 0$ , the dimensional function  $T_c$  assumes a value of 1. The maximum value of  $T_c$  was proposed to 4 at  $\zeta_c = -0.6$ , which implies that two-way cyclic loading with  $\zeta_c = -0.6$  give rise to significantly larger pile rotations than one-way cyclic loading.

In LeBlanc et al. (2010a) also the variation of pile stiffness,  $k = M/\theta$ , was investigated. They found that the pile stiffness increases with the number of load cycles, and further that the increase is independent of factors such as  $\zeta_b$ ,  $\zeta_c$ , and  $I_D$ . It seems questionable that the relative density should have no influence on the increase in pile stiffness. Therefore cyclic tests at higher values of relative density are needed to further extrapolate the findings from LeBlanc et al. (2010a).

LeBlanc et al. (2010b) investigated the accumulated pile rotation for piles exposed to random cyclic loading. They found that the sequence of loading has no significant influence on the accumulated pile rotation. Further, they found that the number of cycles to neutralise  $N$  reversal load cycles is more than  $N$ . Based on that they concluded that conservatively it can be assumed that  $N$  load cycles are necessary to neutralise  $N$  reversal load cycles. Based on the experimental tests they proposed a method to account for random cyclic loading in the determination of the accumulated pile rotation. They suggested to divide a time-series of random cyclic loading into a number of load sequences by means of the extended rainflow method proposed by Rychlik (1987). The accumulated pile rotation of the  $i$ 'th load sequence,  $\theta_i$ , can then be determined by means of the following equations:

$$\Delta\theta_i = ((\Delta\theta_{i-1})^{1/0.31} + (\theta_s T_b T_c)_i^{1/0.31} N_i)^{0.31} \quad (52)$$

$$\theta_i = \Delta\theta_i + \max(\theta_{s,1}, \dots, \theta_{s,i}) \quad (53)$$

where the subscript  $i$  denotes the  $i$ 'th load sequence. The equations are based on the findings in LeBlanc et al. (2010a) and Miner's rule (Miner, 1945).

Achmus et al. (2010a) validated the numerical model proposed by Achmus et al. (2009b) against the small-scale tests reported by LeBlanc et al. (2010a). A reasonable agreement between the numerical model and the experimental findings

were found. However, further validation of the numerical model is needed. It should be noted that the cyclic soil behaviour which they assumed in their numerical model was not based on the sand material employed in the tests by LeBlanc et al. (2010a).

## Summary

The effect of continuous long-term cyclic loading on the accumulated pile rotation/deflection has been investigated experimentally for both slender and non-slender piles. For slender piles several model and field tests have been reported in the literature. The number of load cycles have however for the majority of these tests been less than 100. For non-slender piles the experimental research on the cyclic pile behaviour relies on model tests. The majority of the researchers propose an exponential relationship between the number of cycles and the accumulated pile rotation. However, the research reveals opposing conclusions regarding the effect of the relative density on the exponent relating the pile rotation with the number of cycles.

The effect of continuous long-term cyclic loading on the pile behaviour has been investigated through numerical modelling in which the soil stiffness is degraded based on triaxial tests (Lesny and Hinz, 2007; and Achmus et al., 2009b). The prospect of degrading the soil stiffness in the constitutive models on the basis of triaxial testing is an interesting idea. However, validation against experimental work (preferably field tests) is needed.

Only few experimental pile tests have been conducted regarding the accumulated pile rotation for random long-term cyclic loading. LeBlanc et al. (2010b) found that the accumulated pile rotation is independent of the loading sequence, which disagrees with the findings of Peralta and

Achmus (2010). The influence of loading sequence needs to be further investigated. LeBlanc et al. (2010b) proposed a method for determination of the accumulated pile rotation based on the extended rainflow method proposed by Rychlik (1987) and Miner's rule.

Research regarding the variation of the stiffness of the soil-pile interaction with long-term cyclic loading is needed. Results from LeBlanc et al. (2010a) indicate that the stiffness increases logarithmically with the number of cycles and that the increase is independent of the relative density. However, the tests were only conducted in loose to medium dense soil, and hence a further investigation is needed for dense to very dense soil.

### 4.11 Scour effect on the soil-pile interaction

Around a vertical pile placed on the seabed the water-particle flow from currents and waves will undergo substantial changes causing erosion of soil material. Hence, local scour holes around these piles will form. When large wind farms are built, scouring can also take place on a more global scale. The scour depth of local scour holes can according to DNV (2010) be up to 1.3 times the pile diameter. Scour protection consisting of rock infill can be employed to avoid the development of scour. However, scour protection is very expensive and on some locations it can be hard to deploy due to the sea conditions. Det Norske Veritas provide regulations for the possible depths of global and local scour holes (DNV, 2010). Further, they require that the  $p$ - $y$  curves are modified for the presence of scour. However, they do not provide any regulations on how to modify the  $p$ - $y$  curves for the presence of global and local scour.

The International Organization for Standardization, ISO, and the American

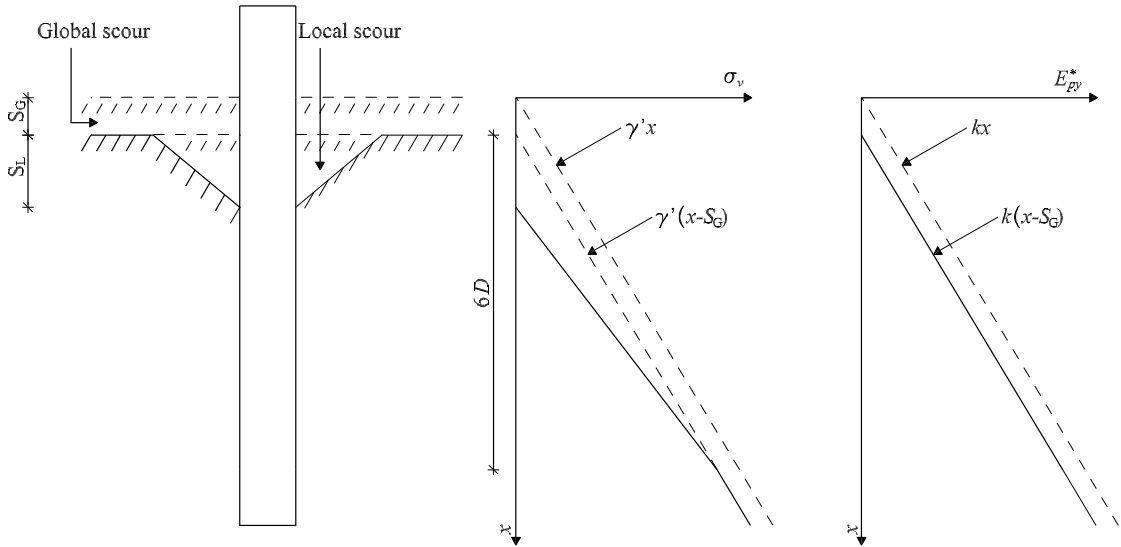


**Figure 29:** Reduction in effective vertical stresses and initial stiffness of the  $p$ - $y$  curves due to global and local scour, after ISO (2007).

Petroleum Institute, API, provides a simple method to account for local and global scour in the  $p$ - $y$  curve formulation (ISO, 2007; API, 2008) in which the effective vertical stresses are assumed to vary with depth as shown in fig. 29. The change in effective vertical stress changes the value of the ultimate soil resistance, cf. (28). They only reduce the initial stiffness of the  $p$ - $y$  curves due to the presence of global scour. In ISO (2007) and API (2008) it is stated that the method shown in fig. 29 is not generally accepted.

When local and global scour takes place, the effective soil stresses decrease. Hence, the soil becomes slightly overconsolidated, with the largest overconsolidation ratio in the upper soil layers. As the soil becomes overconsolidated the soil strength increases. Hence, it is conservative not to take the overconsolidation effect into account. Lin et al. (2010) modified the  $p$ - $y$  curve formulation proposed by Reese et al. (1974) to account for the effect of overconsolidation. Due to the overconsolidation the coefficient of horizontal earth pressure increases, and further, the friction angle increases. These changes in the soil properties were incorporated in the expression of  $p_u$ , cf. (12) and (13). They

compared the pile behaviour calculated by means of a Winkler model approach for the test piles at Mustang Island, cf. Cox et al. (1974), for two conditions: one in which the original friction angle and coefficient of horizontal earth pressure were used; and one in which the overconsolidated parameters were used. They found a significant increase in  $p_u$  when the soil is considered to be overconsolidated. Further, the maximum bending moment in the pile decreased with 7 % when assuming overconsolidated soil. Hence, for piles installed without scour protection, the effect of overconsolidation should be incorporated in the design.

Achmus et al. (2010b) conducted a numerical study of the effect of scour on the lateral pile behaviour of non-slender large-diameter piles. They employed the commercial program ABAQUS and the Mohr-Coulomb constitutive model. They incorporated cyclic soil behaviour by means of the degradation stiffness method (Achmus et al., 2007; Kuo, 2008). They varied parameters such as the pile diameter, the scour depth, and the loading eccentricity. They concluded that, the effect of scour increases for decreasing pile slenderness ratio. Further, they found that scour is more

unfavourable for small loading eccentricities.

Due to changing sea conditions the scour depth around unprotected monopile foundations will vary with time. The process in which the scour depth is decreasing is termed backfilling. Currently, there is no knowledge regarding the properties of the backfilled soil material and how to incorporate this in a Winkler approach. Knowledge regarding these issues are important for the fatigue design of the steel material used for the monopile.

## 5 Conclusion

Monopiles are an often used foundation concept for offshore wind energy converters. They are usually designed by use of the  $p$ - $y$  curve method which is a versatile and practical design method. Furthermore, the method has a long history of approximately 50 years of experience.

The  $p$ - $y$  curve method was originally developed to be used in the offshore oil and gas sector and has been verified for flexible piles with pile diameters up to approximately 2 m. However, for offshore wind turbines, monopiles with diameters of 4 to 6 m and a slenderness ratio around 5 are not unusual.

In the present review a number of the assumptions and not clarified parameters associated with the  $p$ - $y$  curve method have been described. The analyses considered in the review state various conclusions of which some are rather contradictory. Important findings of this paper are summarised as follows:

- When employing the Winkler model approach, the soil response at a given depth is assumed to be independent of the deflections above and below that given depth. Pasternak (1954) proposed a modification of the Winkler model approach in which the shear stress between soil layers is accounted for. However, the effect of involving the shear stress between soil layers seems to be rather small, and from the analysis it is not clear whether the results are dependent on pile properties.
- The failure modes assumed when dealing with the ultimate soil resistance at shallow depth seems rather unrealistic. In the traditionally employed methods the surface of the pile is assumed smooth. Furthermore, the method does not take the pile deflection pattern into account, which seems critical for rigid piles.
- Soil dilatancy affects the soil response such that a large value of the dilatancy angle leads to large values of the ultimate soil resistance. The effect of soil dilatancy is neglected in the  $p$ - $y$  curve formulations. However, a relationship between the soil dilatancy and the friction angle exists. Hence, the influence of soil dilatancy is implicitly accounted for in the expressions for  $p_u$ .
- Determining the ultimate soil resistance by the method proposed by Hansen (1961), seems to give more reasonable results than the method associated with the design codes. Prasad and Chari (1999) presented an expression for the ultimate soil resistance which accounts for the deflection pattern for non-slender piles. Zhang et al. (2005) modified the expression of Prasad and Chari (1999) such that side friction is included. Large-scale tests are needed to further validate the expressions for the ultimate soil resistance.
- In current practice, piles are analysed separately for vertical and horizontal behaviour. The effect on combined loading has until now primarily been

investigated by means of numerical modelling. From this numerical work it can be concluded that vertical loading affects the horizontal pile stiffness and capacity. Compressional vertical loading has a minor positive effect on the horizontal stiffness and capacity, while tensile vertical loading decrease the lateral pile capacity moderately. The effect of combined loading on the vertical stiffness and capacity is more significant.

- Analyses of the sensitivity of  $p$ - $y$  curves to pile bending stiffness,  $E_p I_p$ , gives rather contradictory conclusions. According to the Strain Wedge model, the formulations of  $p$ - $y$  curves are highly affected by the pile bending stiffness. This is in contradiction to the existing  $p$ - $y$  curve formulation and the numerical analyses performed by Fan and Long (2005) as well as Kim and Jeong (2011).
- The initial stiffness is independent of pile diameter according to the existing  $p$ - $y$  curves. This agrees with analytical investigations by Terzaghi (1955), and Vesic (1961). Similarly, Ashford and Juirnarongrit (2005) concluded that initial stiffness is independent of the pile diameter based upon an analysis of a finite element model and tests on large scale concrete piles. Carter (1984) and Ling (1988), however, found that the initial stiffness is linear proportional to pile diameter.
- Based upon a numerical model, Lesny and Wiemann (2006) found that the initial stiffness is over-predicted at large depths when considering non-slender large-diameter piles.
- More research is needed regarding the initial stiffness of  $p$ - $y$  curves.
- Fan and Long (2005) found from numerical analyses that the initial stiffness of the  $p$ - $y$  curves as well as the ultimate soil resistance increases with an increase in the coefficient of horizontal earth pressure. This effect is not taken into consideration in the existing  $p$ - $y$  curve formulations.
- A pile which behaves rigidly will have a negative deflection at the pile toe causing shear stresses at the pile toe. Further, pile rotation at the pile toe will impose a moment on the pile caused by vertical stresses acting on the pile toe. These effects are not taken into consideration in the existing  $p$ - $y$  curve formulations.
- For non-slender, large-diameter piles the research regarding the shape of the  $p$ - $y$  curves is limited.
- The  $p$ - $y$  curves are developed for homogeneous soils. Few analyses have been made on layered soils. Further these analyses have been conducted on flexible piles. Georgiadis (1983) proposed a method to adjust the  $p$ - $y$  curve formulations for layered soils in which an equivalent depth is determined for the soil layers beneath the upper layer. McGann et al. (2012) investigated the effect of layered soil on the  $p$ - $y$  curves and found that both the soil layers above and below an intermediate layer affect the  $p$ - $y$  curves of the intermediate layer. Based on the numerical analyses McGann et al. (2012) proposed a modification of the  $p$ - $y$  curves due to layered soil. Both the findings of Georgiadis (1983) and McGann et al. (2012) needs further validation against tests on non-slender piles.
- Cyclic loading is only in a very simplified manor incorporated in the current  $p$ - $y$  curve formulations. The accumulation of pile deflection due to long-term cyclic loading have been investigated by means of both numerical modelling and small-scale tests. Most researchers conclude that the

pile deflection accumulates exponentially with the number of cycles. Further, factors such as the relative density,  $\zeta_b$  and  $\zeta_c$  affects the accumulation.

- For random cyclic loading LeBlanc et al. (2010b) found that the accumulation of pile deflection is independent of the loading sequency, which is in contrast to the findings of Peralta and Achmus (2010).
- The variation of the stiffness of the soil-pile interaction with cyclic loading needs further investigation. LeBlanc et al. (2010a) suggested that the stiffness increases logarithmically with the number of cycles independently of the relative density of the soil. However, they only considered piles in loose to medium dense sand. Hence, further investigations are needed for piles in dense to very dense sand.
- For piles installed offshore without scour protection both global and local scour will take place. This changes the soil-pile interaction. ISO (2007) suggests a simplified method for modification of  $p$ - $y$  curves due to scouring. However, the method needs validation. Lin et al. (2010) pointed out that the soil becomes overconsolidated when scouring takes place. Hence, the coefficient of horizontal earth pressure and the friction angle increases.
- Due to changing sea conditions the depth of the scour holes around unprotected offshore piles will vary with time. Knowledge is needed regarding the properties of backfilled soil material. Such knowledge can be essential for optimising the fatigue design for monopiles designed unprotected against scour development.

## References

- Abdel-Rahman K., and Achmus M., 2005. Finite element modelling of horizontally loaded Monopile Foundations for Offshore Wind Energy Converters in Germany. *International Symposium on Frontiers in Offshore Geotechnics*, Perth, Australia, Sept. 2005.
- Abdel-Rahman K., and Achmus M., 2006. Numerical modelling of the combined axial and lateral loading of vertical piles. *Proceedings of Numerical Methods in Geotechnical Engineering*, Graz, Austria, Sept. 2006.
- Achmus M., and Thieken K., 2006. Behavior of piles under combined lateral and axial loading. *2nd International Symposium on Frontiers in Offshore Geotechnics*, Perth, Australia, Nov. 2010.
- Achmus M., Abdel-Rahman K., Kuo Y.-S., 2007. Numerical modelling of large diameter steel piles under monotonic and cyclic horizontal loading. *Proceedings of the 10th International Symposium on Numerical Models in Geomechanics*, NUMOG 10, pp. 453-459.
- Achmus M., Abdel-Rahman K., and Thieken K., 2009a. Behavior of Piles in Sand Subjected to Inclined Loads. *Proceedings of International Symposium on Computational Geomechanics*, Juan-Les-Pins, France, May 2009.
- Achmus M., Kuo Y.-S., and Abdel-Rahman K., 2009b. Behavior of monopile foundations under cyclic lateral load. *Computers and Geotechnics*, **36**(5), pp. 725-735.
- Achmus M., Albiker J., and Abdel-Rahman K., 2010a. Investigations on the behavior of large diameter piles under cyclic lateral loading. *Proceeding of Frontiers in Offshore Geotechnics II*, Perth, Western Australia, Australia, pp. 471-476.

- Achmus M., Kuo Y.-S., and Abdel-Rahman K., 2010b. Numerical Investigation of Scour Effect on Lateral Resistance of Windfarm Monopiles. *Proceedings of the Twentieth International Offshore and Polar Engineering Conference*, Beijing, China, June 2010.
- Achmus M., and Thieken K., 2010. Behavior of piles under combined lateral and axial loading. *Proceedings of Frontiers in Offshore Geotechnics II*, Perth, Western Australia, Australia, Nov. 2010, pp. 465-470.
- Alizadeh M., and Davisson M. T., 1970. Lateral load test on piles - Arkansas River project. *Journal of Soil Mechanics and Foundation Engineering Division*, **96**(5), pp. 1583-1604.
- API, 2000. *Recommended practice for planning, designing, and constructing fixed offshore platforms - Working stress design, API RP2A-WSD*, American Petroleum Institute, Washington, D.C., 21. edition.
- API, 2008. *Errata and Supplement 3 for: Recommended Practice for Planning, Designing and Constructing Fixed Offshore Platforms - Working Stress Design*, American Petroleum Institute, Washington, D.C.
- Ashford S. A., and Juirnarongrit T., March 2003. Evaluation of Pile Diameter Effect on Initial Modulus of Subgrade Reaction. *Journal of Geotechnical and Geoenvironmental Engineering*, **129**(3), pp. 234-242.
- Ashford S. A., and Juirnarongrit T., 2005. Effect of Pile Diameter on the Modulus of Subgrade Reaction. *Report No. SSRP-2001/22, Department of Structural Engineering, University of California, San Diego*.
- Ashour M., Norris G., and Pilling P., April 1998. Lateral loading of a pile in layered soil using the strain wedge model. *Journal of Geotechnical and Geoenvironmental Engineering*, **124**(4), paper no. 16004, pp. 303-315.
- Ashour M., and Norris G., May 2000. Modeling lateral soil-pile response based on soil-pile interaction. *Journal of Geotechnical and Geoenvironmental Engineering*, **126**(5), paper no. 19113, pp. 420-428.
- Ashour M., Norris G., and Pilling P., August 2002. Strain wedge model capability of analyzing behavior of laterally loaded isolated piles, drilled shafts and pile groups. *Journal of Bridge Engineering*, **7**(4), pp. 245-254.
- Ashour M., and Norris G., 2003. Lateral loaded pile response in liquefiable soil. *Journal of Geotechnical and Geoenvironmental Engineering*, **129**(5), pp. 404-414.
- Banerjee P. K., and Davis T. G., 1978. The behavior of axially and laterally loaded single piles embedded in non-homogeneous soils. *Geotechnique*, **28**(3), pp. 309-326.
- Barton Y. O., and Finn W. D. L., 1983. Lateral pile response and  $p-y$  curves from centrifuge tests. *Proceedings of the 15th Annual Offshore Technology Conference*, Houston, Texas, paper no. OTC 4502, pp. 503-508.
- Belkhir S., Mezazigh S., and Levacher, D., December 1999. Non-Linear Behavior of Lateral-Loaded Pile Taking into Account the Shear Stress at the Sand. *Geotechnical Testing Journal*, GTJODJ, **22**(4), pp. 308-316.
- Bhattacharya S., Lombardi D., and Wood D. M., 2011. Similitude relationships for physical modelling of monopile-supported offshore wind turbines. *International Journal of Physical Modelling in Geotechnics*, **11**(2), pp. 58-68.
- Bogard D., and Matlock H., 1980. Simplified Calculation of  $p-y$  Curves for Laterally Loaded Piles in Sand. *Unpublished Report*,



- The Earth Technology Corporation, Inc.*, Houston, Texas, USA.
- Briaud J. L., Smith T. D., and Meyer, B. J., 1984. Using pressuremeter curve to design laterally loaded piles. *In Proceedings of the 15th Annual Offshore Technology Conference*, Houston, Texas, paper no. OTC 4501.
- Broms B. B., 1964. Lateral resistance of piles in cohesionless soils. *Journal of Soil Mechanics and Foundation Division*, **90**(3), pp. 123-156.
- Brødbæk, K. T., Augustesen, A. H., Møller, M., and Sørensen, S. P. H., 2011. Physical modelling of large diameter piles in coarse-grained soil. *Proceedings of the 21. European Young Geotechnical Engineers' Conference (XXI EYGEC)*, 4-7. September, Rotterdam, The Netherlands.
- Budhu M., and Davies T., 1987. Nonlinear Analysis of Laterally loaded piles in cohesionless Soils. *Canadian geotechnical journal*, **24**(2), pp. 289-296.
- Carter D. P., 1984. A Non-Linear Soil Model for Predicting Lateral Pile Response. *Rep. No. 359, Civil Engineering Dept., Univ. of Auckland, New Zealand.*
- Comodromos E. M., 2003. Response prediction for horizontally loaded pile groups. *Journal of the Southeast Asian Geotechnical Society*, **34**(2), pp. 123-133.
- Cox W. R., Reese L. C., and Grubbs B. R., 1974. Field Testing of Laterally Loaded Piles in Sand. *Proceedings of the Sixth Annual Offshore Technology Conference*, Houston, Texas, paper no. OTC 2079.
- Das B. M., Seeley G. R., and Raghu D., 1976. Uplift capacity of model piles under oblique loads. *Journal of the Geotechnical Engineering Division*, ASCE, **102**(9), pp. 1009-1013.
- Davisson M. T., and Gill L. C., 1963. Laterally Loaded Piles in a Layered Soil System. *Journal of the Soil Mechanics and Foundation Engineering Division*, ASCE, **89**(SM3), pp. 63-94.
- Davisson M. T. and Salley J. R., 1970. Model study of laterally loaded piles. *Journal of Soil Mechanics and Foundation Engineering Division*, ASCE, **96**(5), pp. 1605-1627.
- Desai C. S., Sharma K. G., Wathugala G. W., and Rigby D. B., 1991. Implementation of hierarchical single surface  $\delta_0$  and  $\delta_1$  models in finite element procedure. *International Journal for Numerical & Analytical Methods in Geomechanics*, **15**(9), pp. 649-680.
- DNV, 2010. *Design of Offshore Wind Turbine Structures, DNV-OS-J101*. Det Norske Veritas, Det Norske Veritas Classification A/S.
- Dobry R., Vincente E., O'Rourke M., and Roesset J., 1982. Stiffness and Damping of Single Piles. *Journal of geotechnical engineering*, **108**(3), pp. 439-458.
- Dordi C. M., 1977. Horizontally Loaded Piles in Layered Soils. *Proceedings of Specialty Session 10, The effect of Horizontal Loads on Piles due to Surcharge of Seismic Effects, Ninth International Conference on Soil Mechanics and Foundation Engineering*, Tokyo, Japan, July 1977, pp. 65-70.
- Dunnavant T. W., and O'Neill M. W., 1985. Performance analysis and interpretation of a lateral load test of a 72-inch-diameter bored pile in overconsolidated clay. *Report UHCE 85-4*, Dept. of Civil Engineering., University of Houston, Texas, p. 57.
- Fan C. C., and Long J. H., 2005. Assessment of existing methods for predicting soil response of laterally loaded piles in sand. *Computers and Geotechnics* **32**, pp. 274-289.
- Georgiadis M., 1983. Development of p-y curves for layered soils. *Proceedings of*

- the Conference on Geotechnical Practice in Offshore Engineering*, ASCE, pp. 536-545.
- Georgiadis M., Anagnostopoulos C., and Safflekou S., 1992. Centrifugal testing of laterally loaded piles in sand. *Canadian Geotechnical Journal*, **29**(2), pp. 208-216.
- Gudehus G., and Hettler A., 1983. Model Studies of Foundations in Granular Soil, *In Development in Soil Mechanics and Foundation Engineering 1*, pp. 29-63.
- Hansen B. J., 1961. The ultimate resistance of rigid piles against transversal forces. *Danish Geotechnical Institute, Bull. No. 12*, Copenhagen, Denmark, 5-9.
- Harremoës P., Ovesen N. K., and Jacobsen H. M., 1984. *Lærebog i geoteknik 2*, 4. edition, 7. printing. Polyteknisk Forlag, Lyngby, Danmark.
- Hetenyi M., 1946. *Beams on Elastic Foundation*. Ann Arbor: The University of Michigan Press.
- Huurman M., 1996. Development of traffic induced permanent strain in concrete block pavements. *Heron*, **41**(1), pp. 29-52.
- ISO, 2007. Petroleum and natural gas industries - Fixed steel offshore structures. *International Organization for Standardization*, ISO 19902:2007 (E).
- Jeong S., Kim Y., and Kim J., 2011. Influence on lateral rigidity of offshore piles using proposed p-y curves. *Ocean Engineering*, **38**(), pp. 397-408.
- Kagawa T., and Kraft L. M., 1980. Lateral load-deflection relationships of piles subjected to dynamic loadings. *Soils and Foundations*, **20**(4), pp. 19-34.
- Karasev O. V., Talanov G. P., and Benda S. F., 1977. Investigation of the work of single situ-cast piles under different load combinations. *Journal of Soil Mechanics and Foundation Engineering*, translated from Russian, **14**(3), pp. 173-177.
- Karthigeyan S., Ramakrishna V. V. G. S. T., and Rajagopal K., May 2006. Influence of vertical load on the lateral response of piles in sand. *Computers and Geotechnics* **33**, pp. 121-131.
- Khadilkar B. S., Chandrasekaran V. S., and Rizvi I. A., 1973. Analysis of Laterally Loaded Piles in Two-Layered Soils. *Proceedings of the Eighth International Conference on Soil Mechanics and Foundation Engineering*, Moscow, Russia, pp. 155-158.
- Kim Y., and Jeong S., 2011. Analysis of soil resistance on laterally loaded piles based on 3D soil-pile interaction. *Computers and Geotechnics*, **38**(2), pp. 248-257.
- Klinkvort R. T., and Hededal O., 2010. Centrifuge modelling of offshore monopile foundations, *Proceedings of International Symposium Frontiers in Offshore Geotechnics 2*, Perth, Western Australia, November 8 to November 10 2010.
- Kuo Y.-S., 2008. On the behavior of large-diameter piles under cyclic lateral load, *Ph.D. thesis Vol. 65*, Leibniz University Hannover, Hannover, Germany.
- LeBlanc C., 2009. Design of offshore wind turbine support structures: Selected topics in the field of geotechnical engineering, *DCE Thesis, Department of Civil Engineering, Aalborg University, Denmark*, (18).
- LeBlanc C., Houlsby G. T., and Byrne B. W., 2010a. Response of Stiff Piles to Long-term Cyclic Loading, *Geotechnique*, **60**(2), pp. 79-90.
- LeBlanc C., Houlsby G. T., and Byrne B. W., 2010b. Response of stiff piles to random two-way lateral loading, *Geotechnique*, **60**(9), pp. 715-721.
- Lesny K., and Wiemann J., 2006. Finite-Element-Modelling of Large Diameter Monopiles for Offshore Wind Energy Converters. *Geo Congress 2006, February 26*

to March 1, Atlanta, GA, USA.

Lesny K., and Hinz P., 2007. Investigation of monopile behaviour under cyclic lateral loading. *Proceedings of Offshore Site Investigation and Geotechnics*, London, England, pp. 383-390.

Lesny K., Paikowsky S. G., and Gurbuz A., 2007. Scale effects in lateral load response of large diameter monopiles. *Geo-Denver 2007 February 18 to 21*, Denver, USA.

Lesny K., and Hinz P., 2009. *Contemporary Topics in Deep Foundations - Proceedings of selected papers of the 2009 International Foundation Congress and Equipment Expo*, pp. 512-519.

Lin S.-S., and Liao J.C., 1999. Permanent Strains of Piles in Sand due to Cyclic Lateral Loads, *Journal of Geotechnical and Geoenvironmental Engineering*, **125**(9), pp. 798-802.

Lin C., Bennett C., Han J., and Parsons R. L., 2010. Scour effects on the response of laterally loaded piles considering stress history of sand, *Computers and Geotechnics*, **37**, pp. 1008-1014.

Ling L. F., 1988. Back Analysis of Lateral Load Test on Piles. *Rep. No. 460, Civil Engineering Dept., Univ. of Auckland, New Zealand*.

Little R. L., and Briaud J. L., 1988a. Cyclic Horizontal Load Test on 6 Piles in Sands at Houston Ship Channel. *Research Report 6540 to USAE Waterways Experiment Station*, Civil Engineering, A&M University, Texas, USA.

Little R. L., and Briaud J. L., 1988b. Full scale cyclic lateral load tests on six single piles in sand. *Miscellaneous Paper GL-88-27*, Geotechnical Division, Texas A&M University, College Station, Texas, USA.

Long J. H., and Vanneste G., 1994. Effects of Cyclic Lateral Loads on Piles in

Sand. *Journal of Geotechnical Engineering*, **120**(1), pp. 225-244.

Matlock H., and Reese L. C., 1960. Generalized Solutions for Laterally Loaded Piles. *Journal of the Soil Mechanics and Foundations Division*, **86**(5), pp. 63-91.

Matlock H., 1970. Correlations for Design of Laterally Loaded Piles in Soft Clay. *Proceedings, Second Annual Offshore Technology Conference*, Houston, Texas, paper no. OTC 1204, pp. 577-594.

McClelland B., and Focht J. A. Jr., 1958. Soil Modulus for Laterally Loaded Piles. *Transactions. ASCE* **123**: pp. 1049-1086.

McGann C. R., Arduino P., and Mackenzie-Helnwein P. (2012). Simplified Procedure to Account for a Weaker Soil Layer in Lateral Load Analysis of Single Piles. *Journal of Geotechnical and Geoenvironmental Engineering*, ASCE, accepted December 14. 2011, posted ahead of print December 17 2011.

Meyerhof G. G., Mathur S. K., and Valsangkar A. J., 1981. Lateral resistance and deflection of rigid wall and piles in layered soils, *Canadian Geotechnical Journal*, **18**, pp. 159-170.

Meyerhof G. G., and Sastry V. V. R. N., 1985. Bearing capacity of rigid piles under eccentric and inclined loads. *Canadian Geotechnical Journal*, (22), pp. 267-276.

Miner M. A., 1945. Cumulative Damage in Fatigue. *Journal of Applied Mechanics*, **12**, pp.A159-A164.

Murchison J. M., and O'Neill M. W, 1984. Evaluation of  $p-y$  relationships in cohesionless soils. *Analysis and Design of Pile Foundations. Proceedings of a Symposium in conjunction with the ASCE National Convention*, pp. 174-191.

Naik T. R., and Peyrot A., 1976. Analysis and Design of Laterally Loaded Piles and Caissons in a Layered Soil System. *Methods of Structural Analysis, Proceedings of*

- the National Structural Engineering Conference*, ASCE, Madison, Wisconsin, USA, Aug. 1976, pp. 589-606.
- Norris G. M., 1986. Theoretically based BEF laterally loaded pile analysis. *Proceedings, Third Int. Conf. on Numerical Methods in offshore piling*, Editions Technip, Paris, France, pp. 361-386.
- O'Neill M. W., Murchison J. M., 1983. An Evaluation of p-y Relationships in Sands. *Research Report No. GT-DF02-83*, Department of Civil Engineering, University of Houston, Houston, Texas, USA.
- O'Neill M. W., and Dunnivant T. W., 1984. A study of effect of scale, velocity, and cyclic degradability on laterally loaded single piles in overconsolidated clay. *Report UHCE 84-7*, Dept. of Civ. Engrg., University of Houston, Texas, p. 368.
- Pasternak P. L., 1954. On a New Method of Analysis of an Elastic Foundation by Means of Two Foundation Constants, *Gosudarstvennoe Izdatelstvo Liberaturni po Stroitelstvu Arkhitekture*, Moskow, pp. 355-421.
- Peck R. B., Hanson W. E., and Thornburn T. H., 1953. *Foundation Engineering*, John Wiley and Sons, Inc. New York.
- Pender M. J., 1993. Aseismic Pile Foundation Design Analysis. *Bull. NZ Nat. Soc. Earthquake Engineering*, **26**(1), pp. 49-160.
- Pender J. M., Carter D. P., and Pranjoto S., 2007. Diameter Effects on Pile Head Lateral Stiffness and Site Investigation Requirements for Pile Foundation Design. *Journal of Earthquake Engineering*, **11**(SUPPL. 1), pp. 1-12.
- Peng J.-R., Clarke B. G., and Rouainia M., 2006. A Device to Cyclic Lateral Loaded Model Piles, *Geotechnical Testing Journal*, **29**(4), pp. 1-7.
- Peralta P., and Achmus M., 2010. An experimental investigation of piles in sand subjected to lateral cyclic loads, *Physical Modelling in Geotechnics*, Taylor & Francis Group, London.
- Petrosowitch G., and Award A., 1972. Ultimate lateral resistance of a rigid pile in cohesionless soil, *Proceedings of the 5th European Conference on SMFE*, Madrid, **3**, pp. 407-412.
- PHRI, 1980. Port and Harbour Research Institute. *Technical Standards for Port and Harbour Facilities in Japan*, Office of Ports and Harbours, Ministry of Transport.
- Poulos H. G., 1971. Behavior of laterally loaded piles: I - Single piles. *Journal of the Soil Mechanics and Foundations Division*, **97**(5), pp. 711-731.
- Poulos H. G., and Davis E. H., 1980. *Pile foundation analysis and design*, John Wiley & Sons.
- Poulos H., and Hull T., 1989. The Role of Analytical Geomechanics in Foundation Engineering. *Foundation Eng.: Current principles and Practices*, **2**, pp. 1578-1606.
- Prakash S., 1962. Behavior of pile groups subjected to lateral loads. *Thesis*, University of Illinois, Urbana, Illinois, USA.
- Prasad Y. V. S. N., and Chari T. R., 1999. Lateral capacity of model rigid piles in cohesionless soils, *Soils and Foundations*, **39**(2), pp. 21-29.
- Reese L. C., and Matlock H., 1956. Non-dimensional Solutions for Laterally Loaded Piles with Soil Modulus Assumed Proportional to Depth. *Proceedings of the eighth Texas conference on soil mechanics and foundation engineering*. Special publication no. 29.
- Reese L. C., Cox W. R., and Koop, F. D., 1974. Analysis of Laterally Loaded Piles in Sand. *Proceedings of the Sixth Annual*

- Offshore Technology Conference*, Houston, Texas, **2**, paper no. OTC 2080.
- Reese L. C., and Welch R. C., 1975. Lateral loading of deep foundation in stiff clay. *Journal of Geotechnic Engineering*, Div., **101**(7), pp. 633-649.
- Reese L. C., and Van Impe W. F., 2001. *Single Piles and Pile Groups Under Lateral Loading*, Taylor & Francis Group plc, London.
- Remaud D., Garnier J., and Frank R. (1998). Laterally loaded piles in dense sand - group effects. *Proceedings of the International Conference Centrifuge*, Tokyo, Japan, pp. 533-538.
- Rycklik I., 1987. A new definition of the rainflow cycle counting method. *International Journal of Fatigue*, **9**(2), pp. 119-121.
- Scott R. F., 1980. Analysis of Centrifuge Pile Tests: Simulation of Pile Driving. *Research Report, American Petroleum Institute OSAPR Project 13*, California Institute of Technology, Pasadena, California, USA.
- Stevens J. B., and Audibert J. M. E., 1979. Re-examination of p-y curve formulation. *Proceedings Of the XI Annual Offshore Technology Conference*, Houston, Texas, OTC 3402, pp. 397-403.
- Stewart H. E., 1986. Permanent strains from cyclic variable-amplitude loadings. *Journal of Geotechnical Engineering*, ASCE, **112**(6), pp. 646-661.
- Sørensen, S. P. H., Brødbæk, K. T., Møller, M., Augustesen, A. H., and Ibsen, L. B., 2009. Evaluation of Load-Displacement Relationships for Large-Diameter Piles. *Proceedings of the twelfth International Conference on Civil, Structural and Environmental Engineering Computing (eds. Topping, Costa Neves and Barros)*, 1.-4. September, Madeira, Portugal, paper 244.
- Sørensen, S. P. H., Ibsen, L. B., and Augustesen, A. H., 2010. Effects of diameter on initial stiffness of  $p$ - $y$  curves for large-diameter piles in sand. *Proceedings of the seventh European Conference on Numerical Methods in Geotechnical Engineering (eds Benz & Nordal eds)*, 2.-4. June, Trondheim, Norway, pp. 907-912
- Terashi M., 1989. Centrifuge modeling of a laterally loaded pile. *Proceedings of the Twelfth International Conference of Soil Mechanics and Foundation Engineering*, Rio de Janeiro, Brazil, pp. 991-994.
- Terzaghi K., 1955. Evaluation of coefficients of subgrade reaction. *Geotechnique*, **5**(4), pp. 297-326.
- Timoshenko S. P., 1941. Strength of materials, part II, advanced theory and problems, 2nd edition, 10th printing. New York: D. Van Nostrand.
- Verdue L., Garnier J., and Levacher D., 2003. Lateral cyclic loading of single piles in sand. *International Journal of Physical Modelling in Geotechnics*, **3**(3), pp. 17-28.
- Vesic A. S., 1961. Beam on Elastic Subgrade and the Winkler's Hypothesis. *Proceedings of the 5th International Conference on Soil Mechanics and Foundation Engineering*, Paris, **1**, pp. 845-850.
- Winkler E., 1867. Die lehre von elasticizitat and festigkeit (on elasticity and fixity), Prague, 182 p.
- Yang Z., and Jeremic B. (2005). Study of Soil Layering Effects on Lateral Loading Behavior of Piles. *Journal of Geotechnical and Geoenvironmental Engineering*, ASCE, **131**(6), pp. 762-770.
- Zhang L., Silva F., and Grismala R., January 2005. Ultimate Lateral Resistance to Piles in Cohesionless Soils. *Journal of Geotechnical and Geoenvironmental Engineering*, **131**(1), pp. 78-83.

## **Recent publications in the DCE Technical Report Series**

Brødbæk K. T., Møller M., Sørensen S. P. H. & Augustesen A. H. 2009. Review of p-y relationships in cohesionless soil. *DCE Technical Report No. 57, Aalborg University, Denmark.*

Sørensen S. P. H., Møller M., Brødbæk K. T., Augustesen A. H. & Ibsen L. B. 2009. Evaluation of Load-Displacement Relationships for Non-Slender Monopiles in Sand. *DCE Technical Report No. 79, Aalborg University, Denmark.*

Sørensen S. P. H., Møller M., Brødbæk K. T., Augustesen A. H. & Ibsen L. B. 2009. Numerical Evaluation of Load-Displacement Relationships for Non-Slender Monopiles in Sand. *DCE Technical Report No. 80, Aalborg University, Denmark.*

Thomassen K., Roesen H. R., Ibsen L. B. & Sørensen S. P. H. 2010. Small-Scale Testing of Laterally Loaded Non-Slender Monopiles in Sand. *DCE Technical Report No. 90, Aalborg University, Denmark.*

Roesen H. R., Thomassen K., Ibsen L. B. & Sørensen S. P. H. 2010. Evaluation of Small-Scale Laterally Loaded Non-Slender Monopiles in Sand. *DCE Technical Report No. 91, Aalborg University, Denmark.*

Sørensen, S. P. H. & Ibsen, L. B. 2011. Small-scale quasi-static tests on non-slender piles situated in sand – Test results. *DCE Technical Report No. 112, Aalborg University, Denmark.*

Sørensen, S. P. H. & Ibsen, L. B. 2011. Small-scale cyclic tests on non-slender piles situated in sand – Test results. *DCE Technical Report No. 118, Aalborg University, Denmark.*

